Toward an Understanding of the High Enantioselectivity in the Osmium-Catalyzed Asymmetric Dihydroxylation (AD). 1. Kinetics

Hartmuth C. Kolb, Pher G. Andersson, and K. Barry Sharpless*

Contribution from the Department of Chemistry, The Scripps Research Institute, 10666 North Torrey Pines Road, La Jolla, California 92037

*Received October 12, 1993**

Abstract: A systematic study of the relationship between ligand structure and saturation rate constants (k_c) in the amine-catalyzed osmylation of terminal olefins was carried out with the aim of learning more about the interactions between the reactants (i.e. OsO_4, the ligand, and the olefin) and of establishing the origin of the large rate accelerations observed with cinchona alkaloid ligands. The results reveal that the saturation rate constants are influenced principally by the nature of the O9 substituent of the cinchona analogs studied, especially if aromatic substrates are used. Additionally, the binding constants (K_{eq}) for OsO_4 and the test ligands were measured, and the observed trends show that K_{eq} can be regarded as an approximate measure of the steric hindrance in the vicinity of the ligand-binding site. Interestingly, the binding constants and the saturation rate constants k_c are not correlated, indicating that the observed rate variations are apparently not caused by variations in ground-state energy due to steric interactions. Rather, the rate data can be interpreted in terms of a relative *stabilization* of the transition state of the reaction in the case of 'fast' ligands. A transition-state stabilization may result from stacking of the olefin and ligand substituents, and this theory is consistent with the fact that flat aromatic substrates give much higher rate constants than aliphatic ones. Further support for this theory was obtained from solvent effect and Hammett studies as well as from X-ray data on osmium glycolate complexes. Phthalazine ligand **1** gives exceptionally high rate constants with aromatic substrates, an effect which can be attributed to the presence of a 'binding pocket', set up by the phthalazine and methoxyquinoline moieties of the ligand, which enables especially good transition-state stabilization for aromatic olefins within the pocket. The enantioselectivity trends were found to parallel the rate trends; therefore, our results allow us to draw conclusions with regard to the mode of chirality transfer in the reaction, leading to a revised mnemonic device.

Introduction

In recent years, the osmium-catalyzed asymmetric dihydroxylation (AD) has experienced considerable improvements in both scope and enantioselectivity.[1] In the course of our ligand optimization study, more than 300 cinchona alkaloid derivatives were tested, and it soon became evident that the enantioselectivity was mainly influenced by the nature of the O9 substituent. More deep-seated structural variations of the alkaloid core had only minor effects on the selectivity.[2] On the basis of this knowledge, we were able to develop two classes of ligands, which complement each other. Alkaloid derivatives **1**,[1a] having a phthalazine substituent at O9, are the most general 'multipurpose' ligands, giving high enantioselectivities for the 1,1- and 1,2-*trans*-disubstituted as well as trisubstituted classes of olefins and for monosubstituted terminal olefins with aromatic substituents. In contrast, a diphenylpyrimidine group on O9 leads to ligands **2**, which are generally superior for terminal olefins, especially those with branching in the substituent.[1b]

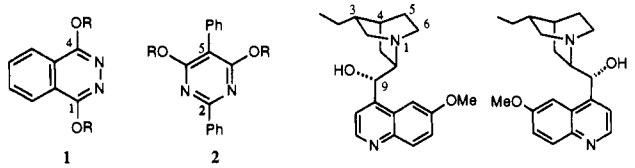

Phthalazine ligands[1a] | Diphenylpyrimidine ligands[1b] | Dihydroquinidine (DHQD) | Dihydroquinine (DHQ)

While attempts have been made to rationalize the origin of face selectivity in the AD reaction,[3] no convincing explanations have been put forward yet.[4] Efforts in this direction are hampered by the lack of mechanistic insight. Currently, two different mechanisms for the osmylation of olefins are being considered: a concerted [3 + 2] cycloaddition mechanism[5] (Figure 1, path A) and a stepwise mechanism which involves the formation and subsequent rearrangement of an osmaoxetane intermediate[6] (path B), formally the product of a [2 + 2] cycloaddition. Our mechanistic investigations suggest a stepwise mechanism,[7] al-

* Abstract published in *Advance ACS Abstracts*. February 1, 1994.

(1) (a) Sharpless, K. B.; Amberg, W.; Bennani, Y. L.; Crispino, G. A.; Hartung, J.; Jeong, K.-S.; Kwong, H.-L.; Morikawa, K.; Wang, Z.-M.; Xu, D.; Zhang, X.-L. *J. Org. Chem.* **1992**, *57*, 2768. (b) Crispino, G. A.; Jeong, K.-S.; Kolb, H. C.; Wang, Z.-M.; Xu, D.; Sharpless, K. B. *J. Org. Chem.* **1993**, *58*, 3785. (c) Sharpless, K. B.; Amberg, W.; Beller, M.; Chen, H.; Hartung, J.; Kawanami, Y.; Lübben, D.; Manoury, E.; Ogino, Y.; Shibata, T.; Ukita, T. *J. Org. Chem.* **1991**, *56*, 4585. (d) For a review, see: Johnson, R. A.; Sharpless, K. B. Catalytic Asymmetric Dihydroxylation. In *Catalytic Asymmetric Synthesis*; Ojima, I., Ed.; VCH: Weinheim, Germany, 1993; pp 227–272. (e) Ogino, Y.; Chen, H.; Kwong, H. L.; Sharpless, K. B. *Tetrahedron Lett.* **1991**, *32*, 3965.

(2) (a) Amberg, W.; Bennani, Y. L.; Chadha, R. K.; Crispino, G. A.; Davis, W. D.; Hartung, J.; Jeong, K.-S.; Ogino, Y.; Shibata, T.; Sharpless, K. B. *J. Org. Chem.* **1993**, *58*, 844. (b) Arrington, M. P.; Bennani, Y. L.; Göbel, T.; Walsh, P. J.; Zhao, S.-H.; Sharpless, K. B. *Tetrahedron Lett.* **1993**, *34*, 7375.

(3) (a) Corey, E. J.; Noe, M. C.; Sarshar, S. *J. Am. Chem. Soc.* **1993**, *115*, 3828. (b) Corey, E. J.; Lotto, G. I. *Tetrahedron Lett.* **1990**, *31*, 2665. (c) Soderquist, J. A.; Rane, A. M. *Tetrahedron Lett.* **1993**, *34*, 5031. (d) Lohray, B. B.; Bhushan, V. *Tetrahedron Lett.* **1992**, *33*, 5113.

(4) Kolb, H. C.; Andersson, P. G.; Bennani, Y. L.; Crispino, G. A.; Jeong, K.-S.; Kwong, H.-L.; Sharpless, K. B. *J. Am. Chem. Soc.* **1993**, *115*, 12226.

(5) (a) Böseken, J. *Recl. Trav. Chim. Pays-Bas* **1922**, *41*, 199. (b) Criegee, R. *Justus Liebig Ann. Chem.* **1936**, *522*, 75. (c) Criegee, R. *Angew. Chem.* **1937**, *50*, 153. (d) Criegee, R. *Angew. Chem.* **1938**, *51*, 519. (e) Criegee, R.; Marchand, B.; Wannowias, H. *Justus Liebig Ann. Chem.* **1942**, *550*, 99.

(6) (a) Sharpless, K. B.; Teranishi, A. Y.; Bäckvall, J.-E. *J. Am. Chem. Soc.* **1977**, *99*, 3120. (b) For reviews, see: Jørgensen, K. A.; Schiott, B. *Chem. Rev.* **1990**, *90*, 1483. (c) Shröder, M. *Chem. Rev.* **1980**, *80*, 187.

(7) (a) Göbel, T.; Sharpless, K. B. *Angew. Chem., Int. Ed. Engl.* **1993**, *32*, 1329. (b) For *ab initio* calculations on possible intermediates, see: Norrby, P.-O.; Kolb, H. C.; Sharpless, K. B. *Organometallics*, in press.

0002-7863/94/1516-1278$04.50/0

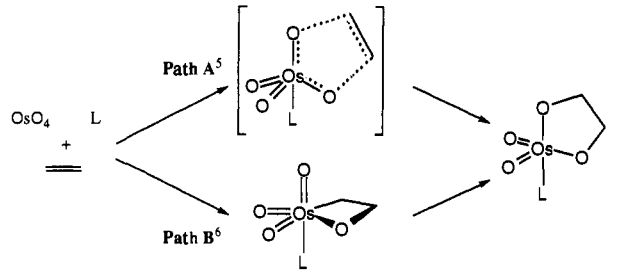

Figure 1. Schematic presentation of the concerted [3 + 2] mechanism (path A) and the stepwise osmaoxetane mechanism[9] (path B).

though definitive evidence for the putative metallaoxetane intermediate is still elusive.[8]

Due to this mechanistic dichotomy, we will discuss the factors governing the relative stability of the transition state as though an osmium·ligand complex was attacked by the olefin in the rate-determining step, as implied by the [3 + 2] mechanism (path A). However, similar arguments can be made for the transition state of the osmaoxetane rearrangement, which is assumed to be rate determining in the stepwise mechanism[9] (path B).

In this paper we present a systematic study of the relationship between ligand structure, binding strength to OsO_4, and reaction rates. The aim of these investigations is to complement our previous enantioselectivity studies and to acquire more direct information on the nature of interactions between ligand and olefin, and ultimately the mode of chirality transfer. Initially, we undertook systematic, step-by-step modifications of the alkaloid moiety in order to determine the structural features responsible for the higher reaction rates obtained with these ligands compared to the parent ligand, quinuclidine itself. We then turned our attention to the influence of the O9 substituent on binding to OsO_4 and on the rate of osmylation.

Preparation of Ligands

Cinchona alkaloid analogs belonging to the following two classes were prepared in racemic form:

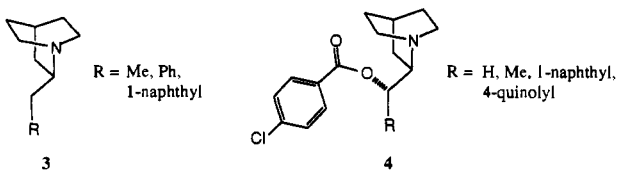

3 4

Quinuclidine derivatives **3** bearing a linear side chain were obtained from 3-quinuclidinone according to known literature procedures[10] in an aldol condensation/hydrogenation/Wolff–Kishner deoxygenation sequence (Scheme 1). The chlorobenzoate ligands of type **4** (R = H, methyl, 1-naphthyl) were synthesized by analogy to literature procedures.[11] Reduction of ethyl quinuclidine-2-carboxylate with $LiAlH_4$ and subsequent esterification gave ligand **4** (R = H). Cinchona analogs **4** (R = methyl, 1-naphthyl) were prepared from 2-cyanoquinuclidine by reaction

Scheme 1[a]

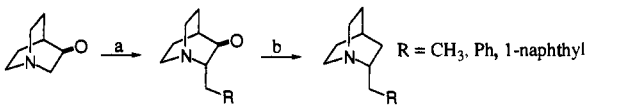

[a] (a) (i) Aldol condensation with RCHO, (ii) H_2/Pd–C; (b) N_2H_4, triethyleneglycol, 155 °C.

Scheme 2[a]

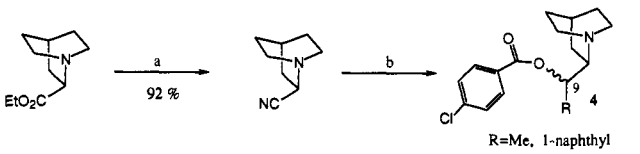

[a] (a) (i) NH_3, MeOH, 120 °C, (ii) triphosgene, pyridine, 0 °C; (b) (i) RMgBr, THF, benzene, reflux, (ii) $LiAlH_4$, THF, reflux for R = Me, or DIBAL, THF, toluene, –78 °C for R = 1-naphthyl, (iii) *p*-Cl-PhCOCl, pyridine.

Scheme 3[a]

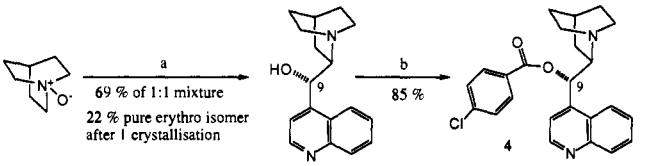

[a] (a) *n*-BuLi, TMEDA, –78 °C, 1 h, then 4-quinolinecarbaldehyde, 1 h, then $TiCl_3$ at room temperature; (b) *p*-Cl-PhCOCl, pyridine.

with the appropriate Grignard reagents, followed by reduction and esterification[11] (Scheme 2).

Condensation of lithiated quinuclidine *N*-oxide and quinoline-4-carboxaldehyde according to an optimized procedure developed in these laboratories[12] (Scheme 3), followed by diastereomer separation and esterification, gave direct access to cinchona analog **4** (R = 4-quinolyl).

Experimental Details for the Kinetic Measurements

Earlier enantioselectivity studies had shown that olefins with aromatic substituents are particularly good substrates for the AD reaction, especially with the phthalazine ligands **1**.[1a] In order to study the effect of aromatic groups, we chose two terminal olefins with aromatic substituents of different size, 2-vinylnaphthalene and styrene, as substrates for our investigations, in addition to 1-decene and vinylcyclohexane as aliphatic controls. The preferred solvent was *t*-BuOH, although solubility problems forced us to change to toluene for cinchona analogs **3** and **4**.

We have previously shown[4] the reaction to obey a rate law which is consistent with either the [2 + 2] or [3 + 2] mechanistic pathways.[5,6] Thus, the reaction is first order in OsO_4 and olefin, but it shows saturation behavior in ligand (Chart 1). The kinetic scheme of the reaction and the corresponding rate law are shown in Scheme 4. The hydrolysis and reoxidation steps of the resulting Os(VI) complex have been omitted from this scheme, since all rate measurements were carried out under stoichiometric conditions. However, the discussions of the factors governing the enantioselectivity of the AD reaction are valid also for the *catalytic* reaction, since the hydrolysis/reoxidation does not affect the selectivity under our biphasic reaction conditions using $K_3Fe(CN)_6$ as the stoichiometric reoxidant.[1c]

It should be noted that the k_1K_{eq} term is larger than k_0 by several orders of magnitude for most quinuclidine and pyridine ligands. As a consequence of this ligand acceleration effect (LAE), the reaction proceeds almost exclusively via the path involving all three components: OsO_4, olefin, *and* ligand. The relationship between the second-order rate constant at complete saturation of the ligand acceleration effect, i.e. the ceiling rate constant k_c, and the microscopic rate constant of the reaction is as follows:

(8) We have not been able to observe a potential osmaoxetane intermediate in a photochemically induced osmylation reaction using matrix isolation techniques: (a) McGrath, D. V.; Brabson, G. D.; Andrews, L.; Sharpless, K. B. Manuscript in preparation. The [2 + 2] and [3 + 2] pathways are kinetically indistinguishable, despite the different mechanistic schemes. (b) For our previous kinetic studies, see ref 4 and: Jacobsen, E. N.; Marko, I.; France, M. B.; Svendsen, J. S.; Sharpless, K. B. *J. Am. Chem. Soc.* **1989**, *111*, 737. (c) Kwong, H.-L. Ph.D. Thesis, Massachusetts Institute of Technology, 1993.

(9) For the application of molecular mechanics calculations in conjunction with an extended MM2* force field for the rationalization of face selectivities based on the osmaoxetane mechanism for the AD reaction, see: Norrby, P. O.; Kolb, H. C.; Sharpless, K. B. Submitted for publication.

(10) Forsyth, D. A.; Prapansiri, V. *J. Am. Chem. Soc.* **1989**, *111*, 4548.

(11) (a) Bulacinski, A. B. *Polish J. Chem.* **1978**, *52*, 2181. (b) Langstrom, B. *Chem. Scr.* **1974**, *5*, 170. (c) Braschler, V.; Grob, C. A.; Kaiser, A. *Helv. Chim. Acta* **1963**, *46*, 2646. (d) Young, J. W. Ph.D. Thesis, Massachusetts Institute of Technology, 1991.

(12) The somewhat difficult isolation of the *N*-oxide condensation product, required by the original procedure (Barton, D. H. R.; Beugelmans, R.; Young, R. N. *Nouv. J. Chim.* **1978**, *2*, 363), was avoided by performing an *in situ* reduction with $TiCl_3$ (see ref 11d). This protocol is easy to carry out, and it also leads to higher yields.

Chart 1. Saturation Plot Obtained with DHQD 9-*O*-*p*-chlorobenzoate (**5**) and Cyclohexene (*t*-BuOH, 25 °C, 680 nm, c_{OsO_4} = 0.000 12 mol/L, $c_{cyclohexene}$ = 0.011 mol/L)

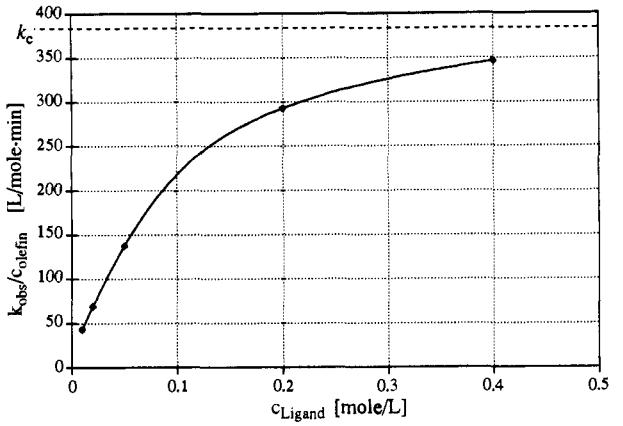

Scheme 4[a]

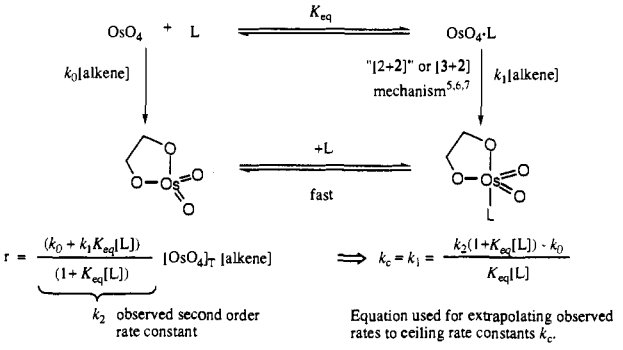

[a] $[OsO_4]_T$ is the total concentration of OsO_4 in the reaction mixture, defined as $[OsO_4]_T = [OsO_4] + [OsO_4 \cdot L]$, and is independent of the ligand concentration.

At saturation $k_1K_{eq}[L] \gg k_0$, and $K_{eq}[L] \gg 1$, so that k_2 (saturation) $\equiv k_c = k_1$. Thus, the ceiling rate constant k_c does not have a K_{eq} component, and it is, therefore, directly related to the activation energy characteristic for each ligand/olefin combination.[13] Consequently, we will discuss *only ceiling rate constants* in this paper. However, in most cases it is not feasible to directly measure saturation rate constants k_c, due to the relatively low binding constants of the cinchona alkaloid ligands as compared to quinuclidine. To circumvent this problem, rate constants k_2 were determined at typically 80–90% ligand saturation and then extrapolated to the ceiling constants k_c using the relationship shown in Scheme 4.[14] The second-order rate constants k_2 were obtained from pseudo-first-order rate constants k_{obs}, which were measured under limiting OsO_4 conditions by monitoring the absorbance of the forming osmium(VI) glycolate monoligand complex (shown in Scheme 4) at 680 nm in a stopped-flow apparatus. Binding constants (K_{eq}) needed for the extrapolation of k_2 were obtained by titrating a solution of the ligand with OsO_4 while monitoring the absorbance of the OsO_4 complex at 400 nm (with *t*-BuOH as solvent) or by following the ^{13}C chemical shifts of the quinuclidine carbons (toluene-d_8 as solvent) and fitting the saturation plot to the 1:1 binding isotherm.[15]

Results and Discussion

Influence of the Alkaloid Structure on Binding and Rate Constants. We were intrigued by the fact that DHQD 9-*O*-*p*-chlorobenzoate (**5**) effects an ca. 8.5 times larger saturation rate constant for styrene in *t*-BuOH as compared to that for quinuclidine, despite its ca. 115 times smaller binding constant. To probe the structural features responsible for the surprisingly large rate acceleration by the alkaloid ligand, a series of modified

(13) The ceiling rate constant k_c is equivalent to the rate constant k_1 of the cycloaddition between ligand–osmium complex and olefin in the [3 + 2] mechanism.

(14) The error in k_c caused by this extrapolation was estimated to be smaller than 5%.

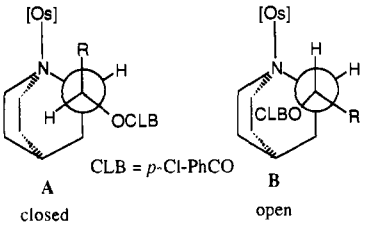

Figure 2. Conformational analysis of the OsO_4 complexes of *erythro* cinchona analogs.[16]

alkaloid surrogates were tested as part of our systematic structure–reactivity–relationship study.

Binding and rate constants were measured in toluene, since the chlorobenzoates of cinchona analogs **4** (R = Me, 1-naphthyl, 4-quinolyl) are considerably less soluble in *t*-BuOH than the parent compounds, e.g. DHQD 9-*O*-*p*-chlorobenzoate (**5**). Thus, the ethyl group on the quinuclidine system and the methoxy substituent of the quinoline moiety enhance the solubility, probably by reducing crystallinity and increasing polarity, respectively.

The binding constants are shown in Chart 2, and the following trends emerged from this study:

(1) Generally, binding of the substituted quinuclidines to OsO_4 requires the ligand to adopt an 'open' conformation B (Figure 2), i.e. a conformation having a hydrogen pointing toward the Os center, in order to reduce steric crowding around the OsO_4 unit. Consequently, the unnatural *threo* isomers, e.g. **8** (K_{eq} = 0.9 L/mol), have lower binding constants than the natural *erythro* isomers, e.g. **9** (K_{eq} = 16.9 L/mol), because the acyloxy and R group switch places, resulting in serious destabilization of the open conformation with the consequence that ligation to OsO_4 is very weak.

(2) K_{eq} is extremely sensitive to steric effects, the general trend being as follows:

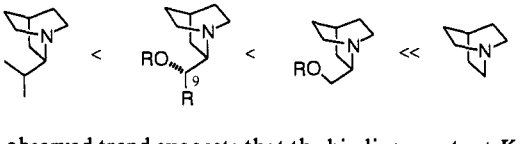

The observed trend suggests that the binding constant K_{eq} can be regarded as a crude measure for the local steric hindrance around the active site of the ligand. Thus, quinuclidine has a binding constant of 80 000 L/mol,[17] and the introduction of a linear substituent, e.g. an ethyl group as in **13**, causes it to drop to 235 L/mol. Branching in the substituent has a disastrous effect on binding; thus, the introduction of a methyl group, as in 2-isopropylquinuclidine, reduces the binding constant to ca. 1 L/mol, while a smaller acyloxy group is somewhat better tolerated (K_{eq} = 7.6 L/mol for a (*p*-chlorobenzoyl)oxy group and *erythro* stereochemistry, i.e. for **6**). Flat, aromatic groups are more favorable than a methyl group, and the binding constants for **9** and **15** are higher than those observed for the corresponding methyl-substituted analogs **6** and **13**, respectively. This is probably

(15) Owing to the presence of two ligating units in $(DHQD)_2PHAL$ (**1**), the 1:1 binding constant K_{eq} could not be accurately determined by UV or NMR methods. The binding and ceiling rate constants for this ligand were obtained as follows. Since each of the two ligating alkaloid units in this ligand acts independently in the reaction,[4] the effective ligand concentration, i.e. its normality, is twice as large as its molarity in the solution. Consequently, $k_2(1 + 2K_{eq}[L])$ versus 2[L] plots are linear (supplementary material) and the slope equals k_cK_{eq}. K_{eq} is the 1:1 binding constant of **1** to OsO_4, and it was determined to be 27.7 L/mol from the plot with 1-decene as substrate (k_c = 1065 L/(mol·min), estimated from the saturation plot, *t*-BuOH, 25 °C). This value for the binding constant was used to extrapolate the second-order rate constants k_2, obtained at ca. 88% saturation, for the other test olefins using 2[L] as the effective ligand concentration.

(16) For a full conformational analysis of cinchona alkaloid esters, see: Dijkstra, G. D. H.; Kellog, R. M.; Wynberg, H.; Svendsen, J. S.; Marko, I.; Sharpless, K. B. *J. Am. Chem. Soc.* **1989**, *111*, 8069.

(17) The binding constant of quinuclidine in toluene was determined in a series of ^{13}C NMR competition experiments with more electron deficient 4-substituted quinuclidines: Kolb, H. C.; Sharpless, K. B. Unpublished results.

Chart 2. Binding Constants in Toluene.

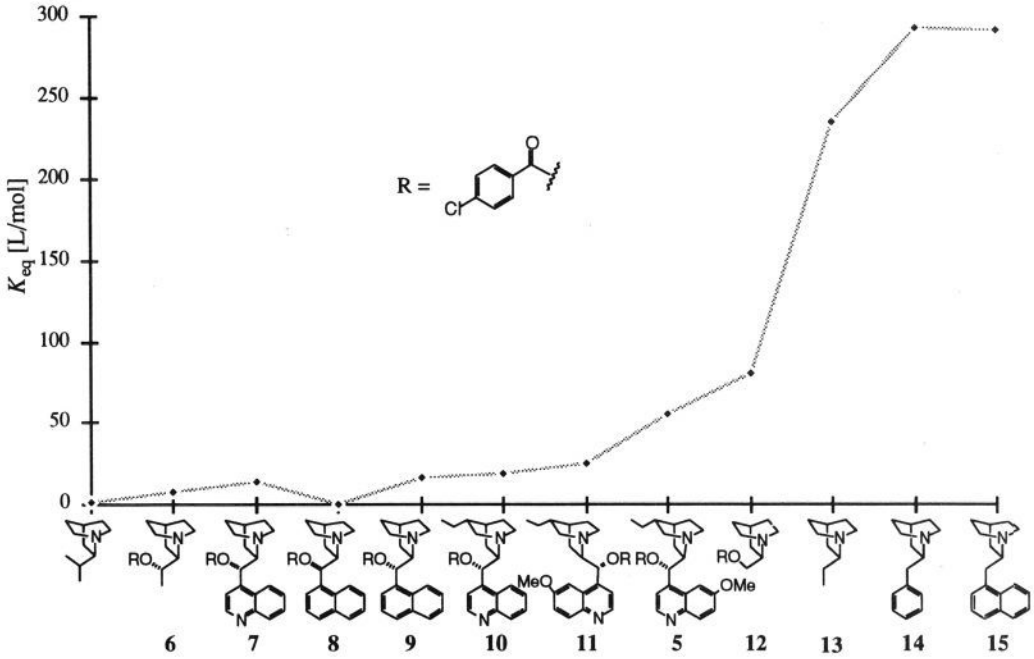

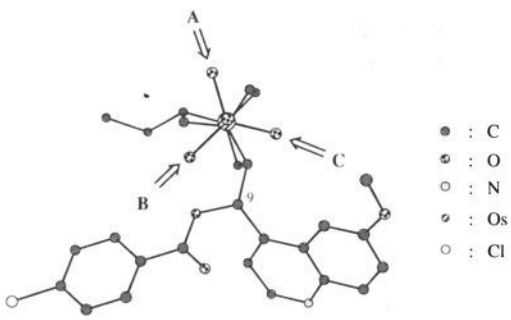

Figure 3. View along the O_{ax}–Os–N axis of the DHQD chlorobenzoate OsO_4 complex.[21]

due to steric effects on the conformational equilibria, since the aromatic group might help to preorganize the ligand for binding to OsO_4 (see Figure 2). Thus, the cinchona alkaloids **11** and **5** are comparatively well set up with regard to binding affinity for OsO_4.

(3) An ethyl group in the quinuclidine moiety, on the bridge carbon C3, distal to the nitrogen, leads to an increase in K_{eq} when it is positioned as in the dihydroquinidine system. Thus, the binding constants are typically lower in the absence of the ethyl group (compare **7** and **10**) or if it is oriented as in the dihydroquinine system (compare **11** and **5**). This may be related to the higher degree of twisting imposed on the quinuclidine ring system by the ethyl group in DHQD analogs, causing one of the two methylene hydrogens to move farther away from the Os center, thereby increasing the binding affinity.[18]

(4) Surprisingly, the methoxy group in the quinoline system has a beneficial effect on the binding constant, despite its close proximity to the OsO_4 unit (see Figure 3). Thus, **5** and **10** have very different binding constants, K_{eq} = 55.6 and 19.5 L/mol, respectively, and yet their structures are very closely related. Molecular mechanics calculations, using the MM2* force field and the continuum solvent model for $CHCl_3$,[19] indicate that both ligands adopt the same conformations and also that the calculated energy requirements for formation of the open, reactive conformations do not explain the observed differences in binding ability ($\Delta E_{o/c}$ = 5.8 kJ/mol for **5**; $\Delta E_{o/c}$ = 4.7 kJ/mol for **10**). At present we can only speculate on the reasons for the larger binding constant of the methoxy-bearing derivative **5**. Perhaps the observed trend is due to stabilizing dipole and van der Waals interactions attributable to the methoxy substituent in the OsO_4 complex of ligand **5**.

The relationship between ceiling rate constants and ligand structure is shown in Chart 3. This plot demonstrates the structural features necessary for high rate accelerations. Generally, aromatic olefins are more sensitive to structural changes of the ligand than aliphatic substrates. The following trends were observed as the fully elaborated structure of the alkaloid system was gradually approached. These trends suggest that specific interactions, which can affect the rate, occur between the substituent on the olefin and the substituents at C9 of the ligand.

(1) Branching in the quinuclidine side chain leads to higher rate constants (Chart 3), despite the detrimental effect on the binding to OsO_4 (Chart 2). Thus, replacing one hydrogen atom in **12** with a methyl group, leading to **6**, causes an ca. 1.85-fold increase in the saturation rate constants for all olefinic test-substrates, and a further increase is observed upon exchanging the methyl for a naphthyl group (cf. **9**). This is probably not due to a simple ground-state destabilizing steric effect, since replacing the acyloxy group in **6** with a methyl group, leading to 2-isopropylquinuclidine, causes a considerable drop in rate.[20] It appears that the combined presence of an oxygenated substituent along with a carbon substituent at C9 is an important 'design element', and the higher rate constants observed with **6** or **9** as compared to **12** are probably partly due to a different

(18) Molecular mechanics calculations, X-ray crystal structure,[33] and NMR experiments[16] indicate that the quinuclidine systems of **10** and **5** are more twisted [$d(N_1–C_6–C_5–C_4)$ = 15.2°] than the quinuclidines of **7** and **11** [$d(N_1–C_6–C_5–C_4)$ = 10.7° and 9.4°, respectively]. See ref 16 for a conformational analysis of the quinuclidine ring system. Molecular mechanics calculations of ligands **5**, **7**, **10**, and **11** were carried out using the MacroModel program in conjunction with the MM2* force field and a continuum solvent model for $CHCl_3$.[19]

(19) (a) MacroModel V3.5X: Mohamadi, F.; Richards, N. G. J.; Guida, W. C.; Liskamp, R.; Caufield, C.; Chang, G.; Hendrickson, T.; Still, W. C. *J. Comput. Chem.* **1990**, *11*, 440. (b) Continuum solvent model: Still, W. C.; Tempczyk, A.; Hawley, R. C.; Hendrickson, T. *J. Am. Chem. Soc.* **1990**, *112*, 6127.

(20) The ceiling rate constants for the osmylation of cyclohexene in toluene, catalyzed by 2-isopropylquinuclidine and 2-ethylquinuclidine (**13**), were measured by monitoring the disappearance of the substrate by GC. Isopropylquinuclidine gives lower saturation rates (k_c = ca. 50 L/(mol·min)) than **13** (k_c = 70 L/(mol·min)), and it is, therefore, also slower than **12** (see Chart 4) and **6**.

Chart 3. Saturation Rate Constants in Toluene at 25 °C

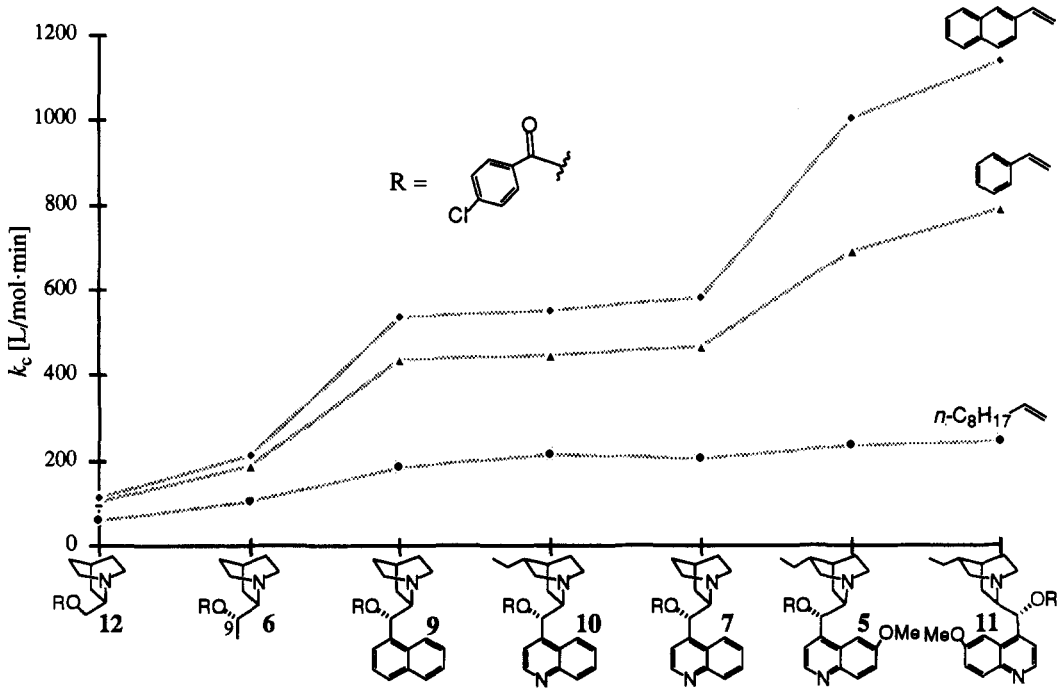

reactive conformation of the OsO_4 complex. In other words, the complex with **12** most likely prefers conformation A (see Figure 2, R = H) so as to minimize steric interactions, while the faster reacting OsO_4 complexes with branched ligands, e.g. **6** or **9**, will prefer conformation B (Figure 2, R = Me, 1-naphthyl). This would suggest that the relative orientation of the O9 substituent has an important influence on the rate.

(2) Although a flat, aromatic group is better than a methyl group (compare **9** and **6** in Chart 3), its electronic character appears to have little influence (compare **9** and **7**). However, a methoxy group on the quinoline system has a beneficial effect on the ceiling rates, resulting in an ca. 1.7 times larger rate constant for 2-vinylnaphthalene (compare **5** and **10**).

(3) The presence of an ethyl group in the quinuclidine moiety is not important for achieving high ceiling rate constants (compare **7** and **10**). However, it enhances the binding affinity to OsO_4 in the dihydroquinidine system (Chart 2) and it increases the solubility of the ligand. Its presence thus represents another important 'design element'.

In summary, the cinchona alkaloid system appears to be ideally set up for the catalytic asymmetric dihydroxylation. The branching in the side chain due to the presence of both a flat, aromatic quinolyl substituent and an oxygenated group in the *erythro* configuration is an essential 'design feature'. Both rate and binding are increased further by the presence of a methoxy group in the quinoline moiety, while the ethyl group on the quinuclidine system enhances the solubility of the ligand and further increases the binding constant for dihydroquinidine derivatives.

(21) The structure of this OsO_4 complex was calculated using our extended MM2* force field.[9] The calculated structure is consistent with NMR experiments carried out earlier.[16] Note that the ligand adopts an 'open' conformation in the complex, i.e., the quinuclidine nitrogen points away from the quinoline ring system (see Figure 2), while the free ligand prefers a 'closed' conformation with the lone pair of the quinuclidine nitrogen positioned above the plane of the quinoline system. For further discussions on the solution conformation of cinchona alkaloids, see ref 16. As shown in Figure 3, the methoxy substituent of the quinoline system probably points toward the Os unit. This is a common structural feature in all our crystal structures of the free ligands,[2] their OsO_4 complexes (Svendsen, J. S.; Markó, I.; Jacobsen, E. N.; Rao, C. P.; Bott, S.; Sharpless, K. B. *J. Org. Chem.* **1989**, *54*, 2263), and their glycolate complexes.[33] The same conformation is probably also preferred in solution, as indicated by the 4 times stronger NOE between the methyl and the proximal *ortho*-proton as compared to the NOE to the distal *ortho*-proton [the NOE experiments were carried out on $(DHQD)_2PHAL$].

The above trends also demonstrate the lack of a direct correlation between ceiling rates and binding to OsO_4. Since K_{eq} can be regarded as a crude measure for the steric bulk around the Os center in the complex (*vide supra*), it follows that the observed trends for the rate constants are difficult to account for based on simple steric interactions. Regardless of the mechanism,[5,6] there are in principle three different low-energy rotamers about the N–O axis for transition-state complexes, consisting of the olefin, ligand, and OsO_4. They formally derive from 'attack' of the olefin along the three directions shown in Figure 3.

Direction A offers the least steric crowding, but it is difficult to see how such an approach can account for the ee and rate variations observed on modifying the C9 substituent. Rather, the sensitivity of the rate constants to the nature of this substituent would suggest directions B or C or be more favorable. This could be as a result of stabilizing interactions between substituents on the olefin and ligand in the transition state of the rate-determining step. The question remains as to which one of these approach directions is favored. The following paragraphs will illustrate the dramatic influence of the O9 substituent on both absolute and relative rate constants for the three test substrates, suggesting that direction B is favored at least in the case of the cinchona-based ligands used in the AD reaction.

Influence of the O9 Substituent on the Ceiling Rate Constant. The above study demonstrates the relationship between ceiling rate and the nature of both substituents at C9. Earlier studies have revealed the sensitivity of the enantioselectivity to the nature of the O9 substituent.[1] This, along with the conformational requirements for the branched quinuclidine side chain (see the first point in the discussion of Chart 3), would suggest that the O9 group plays a central role in the reaction.

Rate and binding constants were measured in *t*-BuOH, since this is the solvent used in the AD reaction. The following trends were observed (Charts 4 and 5):

(1) The order of reactivity of the substrates studied is 2-vinylnaphthalene > styrene > 1-decene ≥ vinylcyclohexane. Interestingly, not only the absolute rate constants but also their ratios, i.e. the chemoselectivities, depend on the ligand structure. With few exceptions,[22] both absolute and relative rates follow the same trends. It should also be pointed out that rates and enantioselectivities are clearly correlated (Table 1).

Chart 4. Saturation Rate Constants in *t*-BuOH at 25 °C

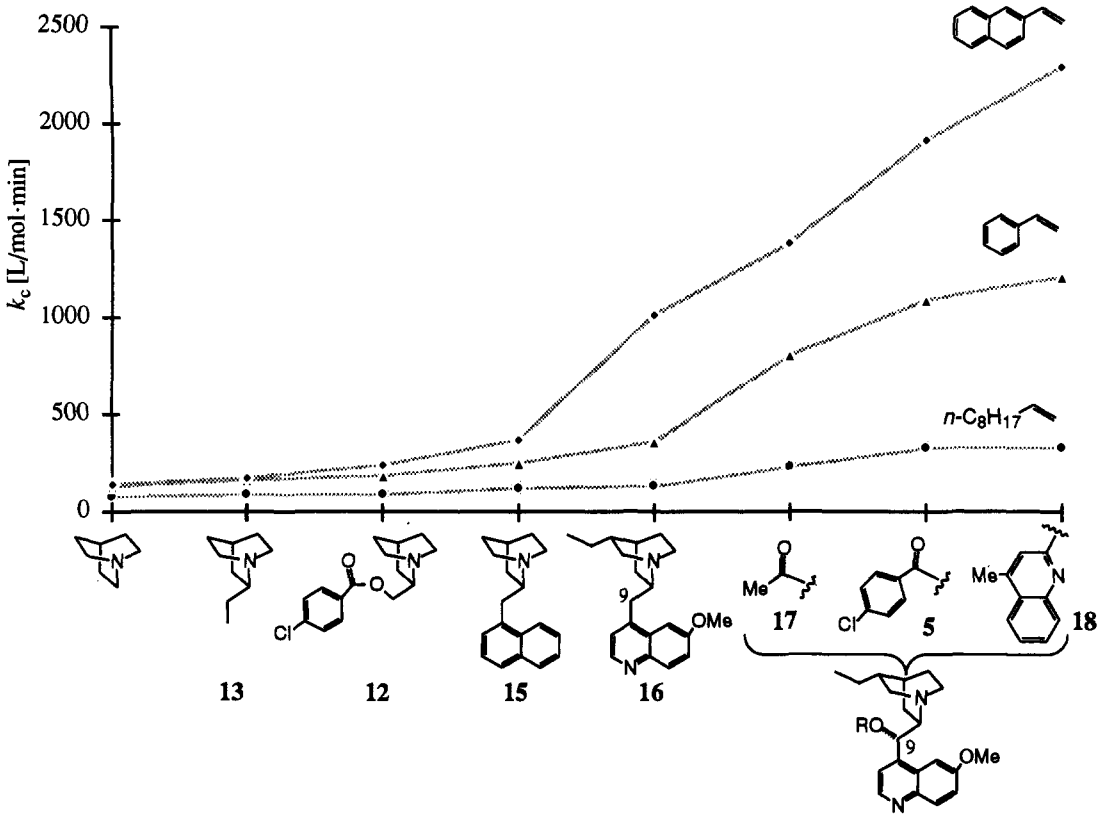

Chart 5. Saturation Rate Constants for Dihydroquinidine Derivatives in *t*-BuOH at 25 °C

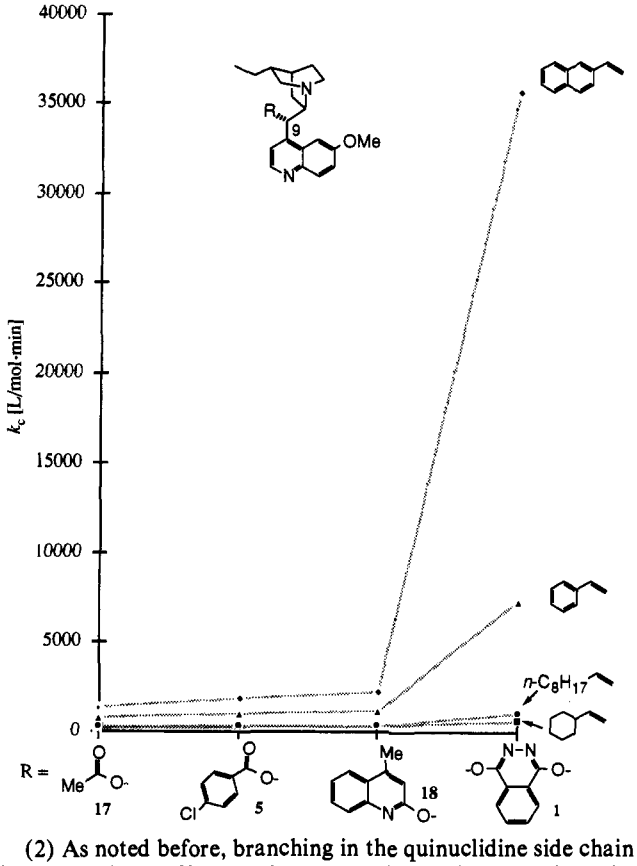

(2) As noted before, branching in the quinuclidine side chain has a beneficial effect on the rates and selectivities. Thus, the rates are constantly low throughout the series of quinuclidines with no branching in the side chain (Chart 4), except for 9-deoxydihydroquinidine (**16**), which shows higher rates than the naphthyl analog **15**, particularly with 2-vinylnaphthalene as the substrate.[23] However, the further introduction of an oxygenated substitutent at C9 in **16** leads to a considerable increase in rate constants, especially if the substituent bears an aromatic group (as in **5** and **18**).

Table 1. Relationship between Enantioselectivities[1] and Ceiling Rate Constants[a]

	n-C8H17					
	%ee	k_c	%ee	k_c	%ee	k_c
5	45[c]	331	74[b] 73[c]	1089	88[c]	1907
18	65[b]	335	87[b]	1210	93[b]	2287
1	84[b]	1065	97[b] 94[c,d]	7320	98[c,d]	35600

[a] Ceiling rate constants k_c [L/(mol·min)] were measured in *t*-BuOH at 25 °C by monitoring the appearance of the glycolate complex at 680 nm in a stopped-flow apparatus; all AD reactions were performed under catalytic conditions in 1:1 *t*-BuOH/H_2O, using $K_3Fe(CN)_6$ as the stoichiometric reoxidant (ref 1). [b] The AD reaction was performed at 0 °C. [c] The AD was carried out at room temperature. [d] Hartung, J.; Sharpless, K. B. Unpublished results.

(3) Not only the enantioselectivities (Table 1) but also the rate constants are very sensitive to the nature of the O9 substituent. While an acetyl group effects only a moderate increase in saturation rates (cf. **16** and **17**), substituents having flat, aromatic groups are much more effective (cf. **5**, **18**, **1**, Charts 4 and 5). Thus, the ceiling rate constants increase in the order Ac < *p*-Cl-PhCO < MEQ ≪ PHAL, and particularly large rate constants are observed with the phthalazine system (cf. **1** and **18**, Chart 5) for aromatic olefins. This would suggest specific rate accelerating

interactions between the O9 substituent and the olefin, and it further implies that the preferred direction of approach brings the olefin close to this substituent.

(4) Also, the relative rate constants depend on the nature of the O9 substituent. While the ceiling rate constants for aliphatic olefins show a relatively small dependence on the ligand structure, aromatic substrates, i.e. styrene and especially 2-vinylnaphthalene, experience a dramatic rate increase, particularly on going from DHQD–MEQ (**18**) to $(DHQD)_2PHAL$ (**1**) (Chart 5). It is noteworthy that vinylcyclohexane, lacking the aromatic substituent found in styrene, is even slower than 1-decene. Hence, there appears to be a beneficial match between flat aromatic groups in both olefin and ligand (*vide infra*). This is most evident for the phthalazine ligand **1**, which also gives uncharacteristically high enantioselectivities for terminal olefins with an *aromatic* substituent (Table 1). For example, the asymmetric dihydroxylation of styrene in the presence of **1** yields the corresponding diol in 97% ee, while vinylcyclohexane gives only 88% ee.[1b]

Discussion. The data shown in Chart 5 demonstrate that the influence of the O9 substituent can be spectacular, leading to much larger rate variations than those caused by changes within the alkaloid core (Chart 4). These observations would suggest that the olefin comes near this substituent in the transition state, i.e. an approach along direction B (see Figure 3), particularly if the ligand has a large, aromatic system at O9.[24] The observed rate acceleration can in principle be explained either by a relative destabilization of the ground state (i.e. the ligand–OsO_4 complex), due to steric effects, or by stabilization of the transition state. The influence of steric effects can be assessed by looking at the binding constants, since K_{eq} can be regarded as a measure of the local steric environment around the OsO_4 unit (*vide supra*). The lack of a correlation between steric effects, i.e. K_{eq}, and ceiling rate constants (Chart 6), in addition to the relatively small influence of the nature of the O9 substituent on K_{eq},[25] makes it seem unlikely that ground-state destabilizing steric effects are the origin of the observed rate trends, since the local steric environment around the Os center is probably very similar for all these ligands.[26]

In contrast, the observed rate (and ee) trends are more consistent with an effect that leads to a stabilization of the transition state. The data reveal that aromatic substrates react faster than aliphatic ones and that increasing the size of the aromatic groups in both ligand and substrate leads to larger ceiling rate constants. Thus,

Chart 6. Saturation Rate Constants versus Binding Constants in *t*-BuOH at 25 °C, Excluding $(DHQD)_2PHAL$ (**1**) and Quinuclidine, Which Are 'Off-Scale' [**1**: K_{eq} = 27.7 L/mol, k_c(2-vinylnaphthalene) = 35 600 L/(mol·min). Quinuclidine: K_{eq} = 2630 L/mol, k_c(vinylnaphthalene) = 147 L/(mol·min)]

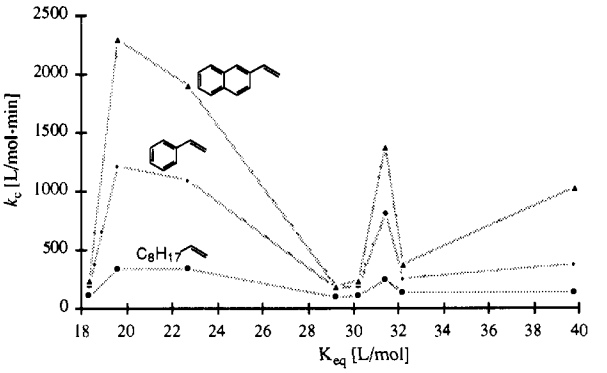

the observed match between flat aromatic groups may be a result of transition-state stabilizing, attractive interactions between these substituents. In accord with this hypothesis, olefins with aliphatic groups are much less responsive to changes in the ligand. Offset-parallel and especially edge-to-face interactions between aromatic groups may be attractive due to van der Waals interactions, solvophobic effects, and dipole interactions.[27] Indeed, Hammett studies with various *para*-substituted benzoate esters, of dihydroquinidine with styrene and the electron-rich *p*-methoxystyrene, as test substrates,[28] suggested that a small electrostatic component is involved. The electron-rich *p*-methoxystyrene reacted slightly faster in the presence of electron-deficient DHQD benzoate derivatives than with electron-rich ones, and the opposite trend was observed for styrene, but the small values of the Hammett reaction constants[28] ($|\rho| < 0.1$) rule out the occurrence of strong orbital interactions, e.g. charge-transfer interactions between the aromatic systems. A Hammett-type correlation between the electronic character of the aromatic system in substituted styrenes and the enantiomeric excess was observed earlier with DHQD-CLB (**5**),[28] electron-donating groups on the substrates leading to an increase in enantioselectivity (ρ = –0.36).

In order to uncover the origins of the exceptionally high rate constants obtained with the phthalazines, particularly for aromatic olefins (see Chart 5), the structure of this ligand was studied more closely. Molecular mechanics calculations as well as NMR experiments with both the free ligand and its bis-osmium complex

(22) Only two ligands have different chemoselectivity pattterns from all the others: 9-deoxydihydroquinidine (**16**) and $(DHQD)_2PYR$ (**2**). The different selectivity behavior observed with these two ligands would indicate that some other rate-determining principles may be involved here. Ligand **16** shows, for this ligand class with no branching at C9, a rather large 2-vinylnaphthalene/styrene rate ratio of k_{rel} = 2.76 in *t*-BuOH, as opposed to the much smaller ratio observed with the closely related ligand **15** (k_{rel} = 1.46) (see Chart 4). Whereas the exact origin of this effect is not clear, the observed sensitivity of the rate constants to the nature of the quinuclidine side chain does suggest that the olefin comes near this side chain in the course of the reaction. The second example occurs with the pyrimidine ligand **2** (the results for this ligand, given below, do not appear in the text), which shows surprisingly large rate constants with 1-decene [k_c = 1458 L/(mol·min), as compared to the rate constant of k_c = 1186 L/(mol·min), observed for 1-decene with $(DHQD)_2PHAL$]. Remarkably, pyrimidine ligand **2**, unlike **1**, does not show much rate increase upon changing from 1-decene to styrene, nor does it distinguish between 2-vinylnaphthalene and styrene (k_c = 2056 L/(mol·min) for styrene, k_c = 2123 L/(mol·min) for 2-vinylnaphthalene). In line with this observation, this ligand gives high enantioselectivities mainly with aliphatic, terminal olefins, while aromatic ones are much poorer substrates.[1b] Molecular mechanics calculations indicate that the observed selectivity behavior of this ligand may originate from its unique conformation. However, this effect remains to be studied in more detail.

(23) Thus, the methoxy substituent of the quinoline moiety and probably to a lesser extent the ethyl group on the quinuclidine system again have a noticeable influence on the absolute and relative rate constants[22] (see also Chart 3 and discussion).

(24) However, direction C also seems to be attainable for ligands that lack the O9 substituent, as indicated by the effect of the methoxy group in this ligand class[22] (compare **15** and **16** in Chart 4).

(25) The binding constants in *t*-BuOH ranged from 19 to 31 L/mol for all the O9-substituted cinchona derivatives studied.

(26) The structures of all ligand–OsO_4 complexes have been calculated using the MacroModel program[19] in conjunction with an extended MM2* force field[9] (e.g., see Figure 3). The calculated structures of the OsO_4 complexes of dihydroquinidine–phthalazine and chlorobenzoate match well with NMR data, including NOE and NOESY experiments, thereby lending credibility to the calculations. All these structures were very similar, showing that the steric environment in the immediate vicinity of the Os center is very similar for all ligands. This is in accord with the observed small dependence of K_{eq} on the nature of the O9 substituent.

(27) Offset parallel interactions become more favorable with increasing size of the arene, which may explain why 2-vinylnaphthalene gives higher saturation rate constants than styrene, see: (a) Jorgensen, W. L.; Severance, D. L. *J. Am. Chem. Soc.* **1990**, *112*, 4768. (b) For a model, which explains the geometric requirements for interactions between aromatic systems, see: Hunter, C. A.; Sanders, J. K. M. *J. Am. Chem. Soc.* **1990**, *112*, 5525. (c) See also: Cozzi, F.; Cinquini, M.; Annunziata, R.; Dwyer, T.; Siegel, J. S. *J. Am. Chem. Soc.* **1992**, *114*, 5729; (d) Cozzi, F.; Cinquini, M.; Annunziata, R.; Siegel, J. S. *J. Am. Chem. Soc.* **1993**, *115*, 5330. For hydrophobic interactions between aliphatic and aromatic groups, see: Liang, G.; Tribolet, R.; Siegel, H. *Inorg. Chem.* **1988**, *27*, 2877.

(28) The Hammett studies were carried out with the *p*-methoxy-, *p*-chloro-, and *p*-nitrobenzoates of DHQD as well as its parent benzoate in *t*-BuOH at 25 °C (see supplementary material). The reaction constants ρ were obtained from $\ln(k_x/k_H)$ plots: styrene, ρ = –0.08; *p*-methoxystyrene, ρ = +0.03. A Hammett-type correlation between the enantioselectivity and the substituent constants σ was obtained earlier with substituted styrenes (ρ = –0.36) and DHQD–CLB (**5**) (ref 8c and: Amberg, W.; Sharpless, K. B. Unpublished results).

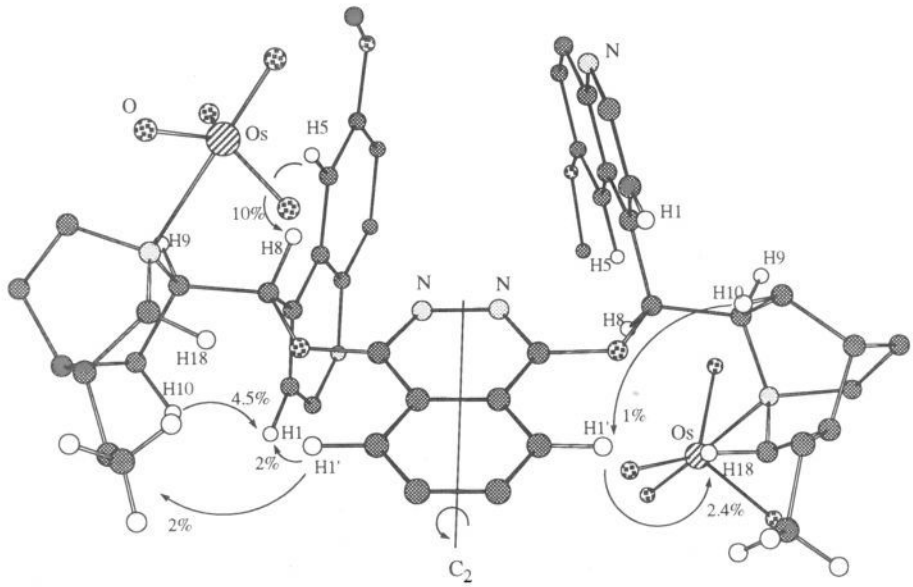

Figure 4. Structure of the bis-OsO_4 complex of $(DHQD)_2PHAL$ based on molecular mechanics calculations and NOE experiments.

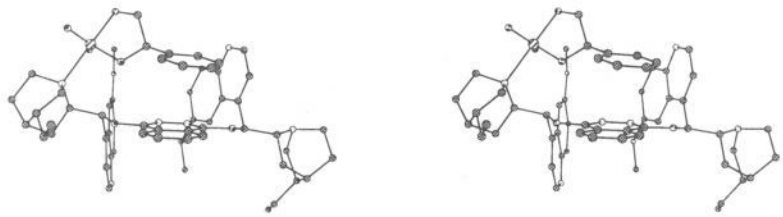

Figure 5. Stereoview of the glycolate complex derived from $(DHQD)_2PHAL$ and styrene.[31]

suggest that $(DHQD)_2PHAL$ (**1**) adopts a solution conformation (see Figure 4) which is similar to that found in the crystal.[2a]

The NMR spectrum of $(DHQD)_2PHAL$ (**1**) shows only one set of signals for the alkaloid moieties, both in the absence and in the presence of excess OsO_4. This would suggest an average C_2-symmetry with respect to an axis through the plane of the phthalazine ring system and therefore a preferred *anti*-arrangement of the two alkaloid units. A series of NOE experiments carried out on the ligand and its bis-OsO_4 complex support this conclusion, and the results are consistent with the relative orientation of the aromatic rings and the quinuclidine units shown in Figure 4. Thus, the complex shows a strong NOE between H5 and H8 (10%), an NOE between H1′ and H1 (2%), and an NOE (2%) between H1′ and the methyl group of the quinuclidine side chain.[29] Similar NOE's were observed for the free ligand, with the exception of the absence of an NOE between H1′ and the ethyl group. As expected, the OsO_4 complex adopts an open conformation (shown in Figure 4), which is supported by the small H8, H9 coupling constant ($J_{8,9} < 1$ Hz, suggesting a dihedral angle of close to 90°) and the NOE's between H10 and H1 (4.5%), H10 and H1′ (1%), and H1′ and H18 (2.4%), as well as the above-mentioned effect between H1′ and the ethyl side chain.[30]

Thus, the quinoline and phthalazine ring systems of $(DHQD)_2$-PHAL (**1**) set up a binding pocket, and an aromatic olefin inside such a pocket would experience not only parallel stacking but also attractive edge-to-face interactions, which may lead to even further stabilization of the transition state and, consequently, higher rates (see Figure 5 for the calculated structure of a glycolate complex;[31] a similar structure has also been calculated for the corresponding osmaoxetane complex[9]). This hypothesis may also account for the extraordinary enantioselectivities obtained with this ligand class for aromatic olefins (Table 1), since chirality transfer based on such effects should be very efficient.[32] For aliphatic substrates, stacking interactions in this same pocket may result from van der Waals and solvophobic effects,[27e] but they will be less effective, leading to lower rates and enantioselectivities.

Seeking further support for this hypothesis, we analyzed the structures of the osmium diolate complexes more closely, since the transition state most likely has some glycolate character and similar principles should be operative in both cases. Molecular mechanics calculations (Figure 5)[9,31] and several X-ray crystal structures (Figure 6) of osmium diolate complexes[33] show the substituents of the glycolate lying right over the O9 substituent, consonant with an approach of the olefin along path **B**.

A comparison of the ^{19}F and ^{1}H NMR variable-temperature NMR spectra of the glycolate complexes derived from *m*-fluo-

(29) In contrast, no NOEs were observed between H1′ and H8 or H5 either in the free ligand or in its OsO_4 complex.

(30) In contrast to the X-ray structure,[2a] which has the two quinuclidines in an *open* conformation, the free ligand in $CDCl_3$ solution seems to adopt a *closed* conformation. (The crystal structure[2a] of $(DHQD)_2PHAL$ is probably influenced by the presence of water molecules within hydrogen-bonding distance of each quinuclidine unit; this may be the cause for the open conformation observed.) Thus, the H8, H9 coupling constant is much larger as compared to that of the OsO_4 complex ($J_{8,9}$ = 6.2 Hz), indicative of a dihedral angle much different from 90°, and NOEs are observed between H18 and H8 (4%) and H10 and H8 (2.5%).

(31) The structure of the glycolate complex was calculated using the MacroModel program[19a] and the extended MM2* force field.[9]

(32) Recent investigations show that both the enantioselectivities and rate constants drop on increasing the size of the substituents of 3,5-disubstituted styrenes, probably because large substituents disfavor the stacked arrangement shown in Figure 5: Loren, S.; Sharpless, K. B. Unpublished results.

(33) (a) X-ray crystal structures were obtained for osmium diolate complexes derived from 3,5-dimethyl-3-hexene and DHQD–CLB (**5**) (Figure 6) as well as the DHQ–CLB analog, see: Pearlstein, R. M.; Blackburn, B. K.; Davis, W. M.; Sharpless, K. B. *Angew. Chem., Int. Ed. Engl.* **1990**, *29*, 639. (b) A similar X-ray was obtained for the glycolate complex derived from 3,5-dimethyl-3-hexene and DHQD 9-*O*-(1-naphthyl) ether: Beller, M.; Davis, W. M.; Sharpless, K. B. Unpublished results. The above X-ray structures demonstrate that the substituents on the ligand and the glycolate adopt a stacked arrangement in the crystal. However, as of yet we have not been able to obtain crystal structures of glycolate complexes derived from *aromatic* olefins and are, therefore, currently undertaking a systematic study to obtain further structural information on complexes involving this class of olefins.

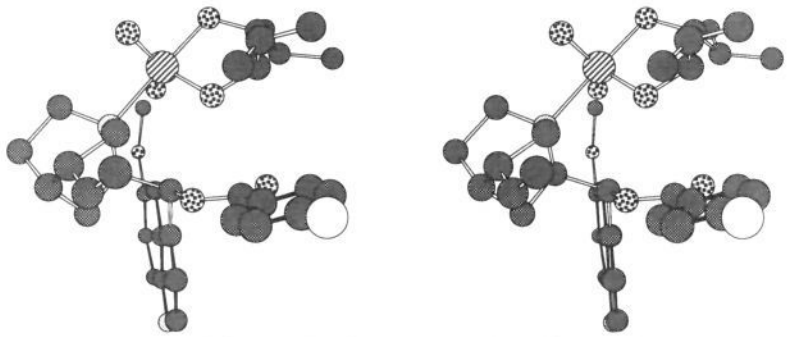

Figure 6. Single crystal X-ray structure (stereoview) of the osmium diolate complex derived from DHQD–CLB (**5**) and 3,5-dimethyl-3-hexene.[33a] A similar structure was obtained with DHQD 9-O-(1-naphthyl) ether as ligand.[33b]

Chart 7. Effect of the Solvent on the Relative Rate Constants

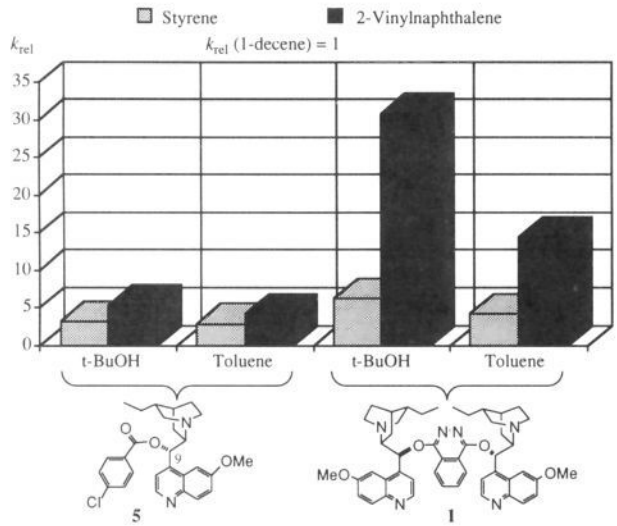

rostyrene and $(DHQD)_2PHAL$ and DHQD 9-O-phenanthryl ether (DHQD–PHN) ligands suggests slower rotation of the phenyl group in the $(DHQD)_2PHAL$ system. Additionally, the ^{19}F signals of the $(DHQD)_2PHAL$ complex are shifted upfield by ca. 0.17 ppm relative to those of the corresponding complex of ethylquinuclidine [at 40 °C], possibly due to the shielding effect of the aromatic group.[34] These results are consistent with the aryl substituent on the glycolate portion of the complex lying in the pocket of the phthalazine ligand (see Figure 5).

This evidence seems to indicate that the glycolates prefer a stacked geometry and that a similar arrangement may also be favorable for the transition state, thereby stabilizing it. Solvent effects may be partially responsible for the stacking, since both ceiling rates as well as relative rates, with respect to 1-decene, drop on changing the solvent from *t*-BuOH to the less polar toluene, probably due to diminished solvophobic effects (see Chart 7). Solvent effects on the enantioselectivity of the system have also been observed, nonpolar solvents having a detrimental effect on the face selectivity.[35]

Strong attractive forces between aromatic systems have been known for some time, and they are assumed to have important effects in biological systems, such as on factors governing protein stability,[36] the structure of DNA,[37] and intercalation of drugs into DNA.[37,38] Also the packing of aromatic molecules in crystals[39] and their aggregation in solution[40] as well as the complexation in many host–guest systems[41] are thought to be partially controlled by attractive aromatic interactions. The idea that stacking interactions influence the selectivity in certain chemical reactions is not new,[42] and they have been invoked to rationalize selectivities in a number of cycloaddition reactions.[43]

The above results are summarized in Figure 7, which demonstrates the relationship between the structure of the ligand and its properties.

These results lead us to revise our mnemonic device[1a] for predicting the stereochemical outcome of the AD reaction (see Figure 8). Earlier we proposed that the southeast quadrant and to a much lesser extent the northwest quadrant of this device presented steric barriers,[1a] whereas the northeast and southwest

(34) Kolb, H. C.; Sharpless, K. B. Unpublished results. The DHQD–PHN complex cannot form a binding "pocket", for it lacks a wall perpendicular to the floor.

(35) Marko, I.; Kolb, H. C.; Sharpless, K. B. Unpublished results.

(36) (a) Burley, S. K.; Petsko, G. A. *Adv. Protein Chem.* **1988**, *39*, 125. (b) Burley, S. K.; Petsko, G. A. *Science* **1985**, *229*, 23. (c) Singh, J.; Thornton, J. M. *FEBS Lett.* **1985**, *191*, 1.

(37) Saenger, W. *Principles of Nucleic Acid Structure*; Springer Verlag: New York, 1984; pp 132–140.

(38) Wakelin, L. P. G. *Med. Res. Rev.* **1986**, *6*, 275.

(39) Desiraju, G. R.; Gavezzotti, A. *J. Chem. Soc., Chem. Commun.* **1989**, 621 and references cited therein.

(40) For examples on porphyrin aggregation, see: (a) Alexander, A. E. *J. Chem. Soc.* **1937**, 1813. (b) Hughes, A. *Proc. R. Soc. London, A* **1936**, *155*, 710. (c) Abraham, R. J.; Eivazi, F.; Pearson, H.; Smith, K. M. *J. Chem. Soc., Chem. Commun.* **1976**, 698. (d) Abraham, R. J.; Eivazi, F.; Pearson, H.; Smith, K. M. *J. Chem. Soc., Chem. Commun.* **1976**, 699.

(41) For some reviews, see the following articles, which appear in: *Frontiers in Supramolecular Organic Chemistry and Photochemistry*; Schneider, H.-J., Dürr, H., Eds.; VCH: Weinheim, Germany, 1991. (a) Schneider, H.-J.; Blatter, T.; Cuber, U.; Juneja, R.; Schiestel, T.; Schneider, U.; Theis, I.; Zimmermann. Shape, Selectivity, and Complementarity in Molecular Recognition. pp 29–56. (b) Diederich, F. Supramolecular Catalysis—Catalytic Cyclophanes. pp 167–191. (c) Stoddart, J. F. Template-Directed Synthesis of New Organic Materials. pp 251–263 and references cited therein. (d) See also: Askew, B.; Ballester, P.; Buhr, C.; Jeong, K.-S.; Jones, S.; Parris, K.; Williams, K.; Rebek, J., Jr. *J. Am. Chem. Soc.* **1989**, *111*, 1082. (e) Williams, K.; Askew, B.; Ballester, P.; Buhr, C.; Jeong, K.-S.; Jones, S.; Rebek, J., Jr. *J. Am. Chem. Soc.* **1989**, *111*, 1090. (f) Lehn, J.-M.; Schmidt, F.; Vigneron, J.-P. *Tetrahedron Lett.* **1988**, *29*, 5255. (g) Zimmerman, S. C.; Wu, W. *J. Am. Chem. Soc.* **1989**, *111*, 8054. (h) Goswami, S.; Hamilton, A. D.; van Engen, D. *J. Am. Chem. Soc.* **1989**, *111*, 3425. (i) Sijbesma, R. P.; Kentgens, A. P. M.; Nolte, R. J. M. *J. Org. Chem.* **1991**, *56*, 3199. (j) Shepodd, T. J.; Petti, M. A.; Dougherty, D. A. *J. Am. Chem. Soc.* **1988**, *110*, 1983. (k) Kumpf, R. A.; Dougherty, D. A. *Science* **1993**, *261*, 1708. (l) Stauffer, D. A.; Dougherty, D. A. *Tetrahedron Lett.* **1988**, *29*, 6039. (m) Stauffer, D. A.; Dougherty, D. A. *Science* **1990**, *250*, 1558.

(42) For example, attractive aromatic interactions between fullerene surfaces and the phenanthryl units of DHQD–PHN have been invoked to rationalize the high efficiency of this ligand in the kinetic resolution of fullerenes, see: (a) Hawkins, J. M.; Meyer, A.; Nambu, M. *J. Am. Chem. Soc.*, **1993**, *21*, 9844. (b) Hawkins, J. M.; Meyer, A. *Science* **1993**, *260*, 1918.

(43) For the influence of attractive interactions between a dienophile and Lewis-acid catalyst on the enantioselectivity of Diels–Alder reactions, see: (a) Hawkins, J. M.; Loren, S. *J. Am. Chem. Soc.* **1991**, *113*, 7794. (b) Hawkins, J. M.; Loren, S.; Nambu, M. *J. Am. Chem. Soc.*, in press. (c) Corey, E. J.; Loh, T.-P.; Roper, T. D.; Azimioara, M. D.; Noe, M. C. *J. Am. Chem. Soc.* **1992**, *114*, 8290. (d) Corey, E. J.; Matsumura, Y. *Tetrahedron Lett.* **1991**, *32*, 6289. π–π-interactions between dienophiles and aromatic rings in covalently bound chiral auxiliaries have been proposed for several asymmetric Diels–Alder reactions, see: Evans, D. A.; Chapman, K. T.; Bisaha, J. *J. Am. Chem. Soc.* **1988**, *110*, 1238 and references therein. (f) For the influence of aromatic stacking interactions on the regioselectivity in the platinum-catalyzed hydroformylation reaction, see: Castonguay, L. A.; Rappé, A. K.; Casewit, C. J. *J. Am. Chem. Soc.* **1991**, *113*, 7177.

(44) Recent investigations indicate that hydroxymethyl groups can be positioned here with positive effects on both rate and enantioselectivity, possibly due to hydrogen bonding to an oxo-group on osmium: van Nieuwenhze, M.; Sharpless, K. B. *Tetrahedron Lett.*, in press.

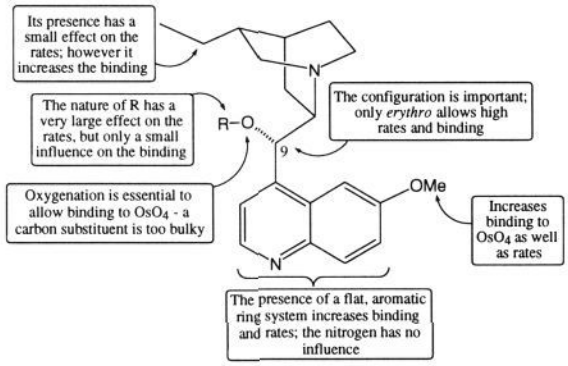

Figure 7. Relationship between ligand structure and K_{eq} and ceiling rate constants. The alkaloid core is ideally set up to ensure high rates, binding, and solubility. The rates are influenced considerably by the nature of the O9 substituent, while the binding to OsO_4 is almost independent of that substituent.

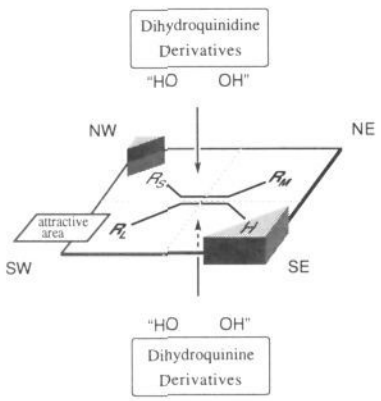

Figure 8. Mnemonic device for rationalizing the face selectivity.

quadrants were relatively open. An olefin, positioned according to these constraints, will be attacked either from the top face, in the case of DHQD derivatives, or from the bottom face, in the case of DHQ derivatives. Our current results indicate that this mnemonic device will be more useful if modified so that the southwest quadrant in this scheme is regarded as being an *attractive* area, especially well suited to accommodate flat aromatic substituents. This new view is to replace the earlier one, which represented the southwest quadrant as an open, i.e. sterically neutral, area. The northeast and southeast quadrants retain their original labels: open and severely crowded, respectively. The northwest quadrant is still considered to exhibit modest steric restriction, but it now appears that it can also play an attractive role for a special class of olefinic substrates.[44] Currently, molecular mechanics models are being developed on the basis of the above findings as well as of *ab initio* calculations.[9,45]

Conclusions

The above systematic study has led to a better understanding of the nature of the interactions between ligand and substrate and also of the origins of the large rate acceleration observed with the cinchona alkaloid derivatives used in the AD reaction. Generally, rate constants and enantioselectivities follow similar trends. These trends cannot be easily explained on the basis of steric interactions between the substituents on the olefin and the ligand. Rather, a stabilizing interaction resulting from stacking of these substituents in the transition state may be responsible for the considerable influence of the O9 substituent on the ceiling rates. Such an effect would have important consequences with regard to the enantioselectivity, since it brings an olefin substituent into close proximity to the stereogenic centers in the ligand. An approach along direction **A** (Figure 3), i.e. farther away from the chiral environment, is unlikely to lead to high enantioselectivities and seems inconsistent in view of the large influence of the O9 substituent on both rate and selectivity. The phthalazine ligands appear to be especially well suited to 'recognize' flat, aromatic olefins, probably because such olefins fit optimally into the pocket set up by the aromatic ring systems of the ligand (Figure 5). A model for rationalizing the face selectivity in the AD reaction is currently under development.[9,45]

In summary, while the enantioselectivities and the saturation rates are greatly influenced by the nature of the O9 substituent, the cinchona alkaloid backbone provides an almost perfect set of solubility and binding characteristics to serve as the ligand in these osmium-catalyzed asymmetric dihydroxylations.

Experimental Section

General Methods. The kinetic measurements were carried out at 25 °C under pseudo-first-order conditions (limiting OsO_4) by following the formation of the osmium glycolate at 680 nm in a HI-Tech Scientific stopped-flow apparatus. Melting points are uncorrected. ^1H and ^{13}C NMR spectra were recorded in $CDCl_3$ at 400 and 100 MHz, respectively. All ^1H NMR coupling values are given in hertz. IR spectra were recorded on a Nicolet 510 FT-IR spectrometer. All solvents were purified and dried according to standard methods. Analytical TLC was performed with precoated aluminum TLC plates (silica gel 60 F_{254}, layer thickness 0.2 mm, E. Merck, Darmstadt, Germany). Preparative flash chromatography was performed using Merck silica gel 60 (230–400 mesh).

All of the synthetic alkaloid analogs were prepared and used in racemic form.

2-Acetylquinuclidine. A two-necked flask, equipped with a reflux condenser and pressure-equalizing dropping funnel, was charged with benzene (20 mL) and MeMgBr (3M solution in ether, 13 mL, 39 mmol) under an atmosphere of argon. A solution of 2-cyanoquinuclidine[11] (2.5 g, 18.36 mmol) in benzene (30 mL) was added dropwise, and the mixture was heated at reflux for 3 h. After the mixture was cooled to room temperature, the reaction was quenched with saturated aqueous NH_4Cl (10 mL), and the mixture diluted with H_2O (10 mL) and acidified with concentrated HCl (10 mL), while stirring vigorously. The organic layer was separated and extracted with 2M HCl (3 × 50 mL), and the aqueous layers were combined. After the aqueous phase was heated at 40 °C for 1 h, H_2O and acid were evaporated *in vacuo* and the residue was dissolved in H_2O (70 mL). The solution was basified with K_2CO_3, causing the formation of a white precipitate (MgO), and then extracted with ether (4 × 50 mL). The extracts were dried (K_2CO_3) and evaporated under vacuum. Vacuum distillation of the residue gave 2-acetylquinuclidine (2.5 g, 89%) as a colorless liquid: bp 45–47 °C (0.2 mmHg); IR (neat) ν 2954 (s), 2861 (s), 1708 (s), 1457 (m), 1356 (s), 1189 (s), 1059 (m), 957 (m), 810 (m), 608 (m), 561 (m) cm^{-1}; ^1H NMR δ 3.28 (ddd, J = 1.6, 7.3, 10.2, 1H), 3.01–2.83 (m, 2H), 2.73–2.64 (m, 1H), 2.58–2.49 (m, 1H), 2.17 (s, 3H), 1.92 (ddt, J = 7.3, 13.1, 2.2, 1H), 1.78 (hept, J = 3.2, 1H), 1.55–1.42 (m, 3H), 1.38–1.32 (m, 2H); ^{13}C NMR δ 209.4 (CO), 65.4 (CH), 49.2 (CH_2), 44.0 (CH_2), 27.7 (CH_3), 26.5 (CH_2), 26.0 (CH_2), 25.8 (CH_2), 21.3 (CH); MS (FAB$^+$/NBA) calculated for $C_9H_{16}NO$ (MH^+), 154.1232; found, 154.1230.

***threo*- and *erythro*-2-(1-Hydroxyethyl)quinuclidine *p*-Chlorobenzoate.** A two-necked flask, equipped with a reflux condenser and a pressure-equalizing dropping funnel, was charged with $LiAlH_4$ (0.6 g, 15.81 mmol) and anhydrous THF (28 mL) under argon. A solution of 2-acetylquinuclidine (2.45 g, 15.96 mmol) in THF (15 mL) was added dropwise, and the mixture was heated at reflux for 45 min and then cooled to room temperature and quenched by careful addition of H_2O (0.8 mL), causing the

(45) While our own efforts are based on a stepwise osmaoxetane mechanism, Houk's group is currently developing a molecular mechanics model based on the [3 + 2] mechanism: Niwayama, S.; Houk, K. N. Private communication.
(46) Pluim, H. Ph.D. Thesis, Rijksuniversiteit te Groningen, 1982.

formation of a gel. Solid $NaHCO_3$ was added and the mixture stirred for ca. 30 min to break up the gel; then the mixture was filtered through a pad of Celite, and the pad was washed with copious amounts of ether. The filtrate was evaporated *in vacuo* to give the crude alcohol (2.3 g, 93%) as a 3:1 mixture of *threo* and *erythro* diastereomers. The crude mixture of alcohols was used directly for the subsequent esterification without further purification. Pyridine (1.15 mL, 14.2 mmol) was added to a solution of the alcohol (2.23 g, 14.33 mmol) in CH_2Cl_2 (25 mL) at 0 °C, followed by *p*-chlorobenzoyl chloride (1.95 mL, 15.34 mmol). The solution was warmed to room temperature and the reaction quenched after 1 h by addition of H_2O (1 mL) and stirring for a further 30 min. The reaction mixture was washed with 2 M K_2CO_3 (80 mL), and the aqueous layer was reextracted with CH_2Cl_2 (3 × 80 mL). The combined organic layers were dried (K_2CO_3) and evaporated *in vacuo*. Flash chromatography (silica gel, ethyl acetate/ethanol/Et_3N, 90:8:2) of the residue gave the less polar *threo*-2-(1-hydroxyethyl)quinuclidine *p*-chlorobenzoate (3.02 g, 64%) as a colorless oil and the more polar *erythro* isomer **6** (0.85 g, 18%) as colorless needles. The relative configuration of the *erythro* compound **6** was established by single-crystal X-ray diffraction (supplementary material). Physical data for the *threo* isomer: IR (neat) ν 2933 (s), 2865 (m), 1715 (s), 1594 (m), 1275 (s), 1106 (m), 1090 (m), 1015 (m), 758 (m) cm^{-1}; ^1H NMR δ 7.96 (d, J = 8.7, 2H), 7.38 (d, J = 8.7, 2H), 5.21 (dq, J = 9.0, 6.3, 1H), 3.13–3.03 (m, 1H), 2.92–2.83 (m, 3H), 2.72–2.62 (m, 1H), 1.81 (m, 1H), 1.71 (dddd, J = 1.7, 4.4, 9.5, 12.7, 1H), 1.55–1.47 (m, 2H), 1.47–1.40 (m, 2H), 1.31 (d, J = 6.3, 3H), 1.20–1.12 (m, 1H); ^{13}C NMR δ 165.4 (CO), 138.9 (Cq), 131.1 (2CH), 129.3 (Cq), 128.5 (2CH), 71.3 (CH), 60.2 (CH), 49.7 (CH_2), 42.1 (CH_2), 30.1 (CH_2), 26.6 (CH_2), 25.5 (CH_2), 21.6 (CH), 17.2 (CH_3); MS (FAB$^+$/NBA) calculated for $C_{16}H_{21}ClNO_2$ (MH^+), 294.1261; found, 294.1260. Physical data for the *erythro* isomer: mp 75 °C; IR (KBr) ν 3031 (w), 2944 (m), 2867 (m), 1711 (s), 1594 (m), 1275 (s), 1108 (m), 1084 (m), 760 (m) cm^{-1}; ^1H NMR δ 7.97 (d, J = 8.8, 2H), 7.41 (d, J = 8.6, 2H), 5.19 (dq, J = 9.3, 6.2, 1H), 2.99–2.83 (m, 4H), 2.72 (dt, J = 13.9, 7.7, 1H), 1.82–1.71 (m, 2H), 1.57–1.44 (m, 4H), 1.39 (d, J = 6.1, 3H), 1.29 (br dd, J = 7.9, 11.9, 1H); ^{13}C NMR δ 165.4 (CO), 139.3 (Cq), 130.9 (2CH), 129.1 (Cq), 128.7 (2CH), 74.6 (CH), 60.1 (CH), 50.3 (CH_2), 42.4 (CH_2), 30.8 (CH_2), 26.6 (CH_2), 25.7 (CH_2), 21.3 (CH), 19.0 (CH_3); MS (FAB$^+$/NBA) calculated for $C_{16}H_{21}ClNO_2$ (MH^+), 294.1261; found, 294.1260.

(2-Quinuclidinyl) (1-Naphthyl) Ketone. A dry three-necked round-bottomed flask equipped with a reflux condenser with an argon inlet and a pressure-equalizing dropping funnel was charged with magnesium turnings (0.75 g, 30.9 mmol) and anhydrous THF (15 mL). 1-Bromonaphthalene (4.09 mL, 29.4 mmol) was added dropwise, and the mixture was warmed initially to start the formation of the Grignard reagent. After completion of the addition, the dark reaction mixture was heated at reflux for 3 h and then allowed to cool to room temperature. A solution of 2-cyanoquinuclidine[11] (2.00 g, 14.7 mmol) in benzene (10 mL) was added to the Grignard reagent, and the mixture was heated at reflux. After 3 h, the reaction was cooled in an ice bath and then quenched by first adding 10 mL of saturated aqueous NH_4Cl dropwise and then pouring the mixture into 30 mL of saturated NH_4Cl. The flask was rinsed with water and benzene and the mixture acidified with concentrated HCl (10 mL). The layers were separated, and the organic phase was extracted with 2N HCl (2 × 25 mL). The combined aqueous extracts were warmed to ca. 40 °C for 2 h and then evaporated *in vacuo*. The residue was taken up with water (30 mL), made alkaline with saturated K_2CO_3 solution, and extracted with ether (4 × 50 mL). The organic extracts were dried (K_2CO_3) and evaporated under vacuum to afford the crude ketone as a yellowish solid (3.32 g, 85%), which was spectroscopically identical to the compound prepared previously:[11d,46] ^1H NMR δ 8.43 (br d, J = 9.0, 1H), 7.95 (d, J = 8.3, 1H), 7.90 (dd, J = 1.1, 7.2, 1H), 7.86 (dd, J = 1.4, 8.0, 1H), 7.59–7.46 (m, 3H), 4.36 (ddd, J = 0.9, 7.5, 10.3, 1H), 3.16–3.07 (m, 1H), 3.04–2.92 (m, 2H), 2.73 (dddd, J = 1.5, 4.1, 10.6, 14.0, 1H), 2.17 (ddt, J = 7.6, 13.1, 2.1, 1H), 1.93 (sept, J = 2.8, 1H), 1.73–1.54 (m, 4H), 1.52–1.42 (m, 1H).

***erythro*- and *threo*-2-[Hydroxy(1-naphthyl)methyl]quinuclidine.** Diisobutylaluminum hydride (1.5 M solution in toluene, 9.5 mL, 14.3 mmol) was added dropwise to a solution of (2-quinuclidinyl) (1-naphthyl) ketone (2.92 g, 11.0 mmol) in toluene (30 mL) and THF (12 mL) at −78 °C under argon. The solution was stirred at −78 °C for 3 h and then allowed to warm to room temperature overnight. After the reaction was quenched by careful addition of water (1.0 mL), the mixture was diluted with ethyl acetate (50 mL) and solid $NaHCO_3$ was added while stirring vigorously until the precipitate turned granular. After 30 min, the mixture was filtered and the residue washed with warm ethyl acetate (200 mL). The filtrate was evaporated to obtain the crude alcohol as a colorless solid (2.88 g, 98%). Recrystallization of the crude product from toluene (10 mL) gave the pure *erythro* isomer (0.87 g, 30%) as colorless, fine needles. The mother liquor was evaporated and contained mainly the *threo* isomer (1.86 g), which was used without further purification. The stereochemistry was assigned on the basis of spectroscopic similarities to related compounds.[11d] Physical data for *erythro*-2-[hydroxy(1-naphthyl)methyl]quinuclidine: mp 199 °C (lit.[11d] 198.5–200 °C); IR (KBr) ν 3200–2400 (br, OH), 2941 (s), 2912 (m), 2867 (m), 1596 (w), 1511 (m), 1455 (m), 1129 (m), 990 (m), 816 (m), 783 (s) cm^{-1}; ^1H NMR δ 8.05 (d, J = 8.3, 1H), 7.86 (br d, J = 8.6, 1H), 7.76 (d, J = 8.2, 1H), 7.73 (d, J = 7.1, 1H), 7.49–7.37 (m, 3H), 5.81 (d, J = 3.6, 1H), 4.06 (br s, OH), 3.62–3.51 (m, 1H), 3.16 (dt, J = 3.8, 8.8, 1H), 2.94–2.84 (m, 1H), 2.73 (ddd, J = 7.3, 9.7, 13.3, 1H), 2.55–2.45 (m, 1H), 1.94–1.77 (m, 2H), 1.66–1.55 (m, 1H), 1.47–1.24 (m, 4H); ^{13}C NMR δ 139.7 (Cq), 133.7 (Cq), 130.4 (Cq), 128.8 (CH), 127.7 (CH), 126.0 (CH), 125.3 (2CH), 123.5 (CH), 123.1 (CH), 72.6 (CH), 59.9 (CH), 50.6 (CH_2), 43.8 (CH_2), 26.5 (CH_2), 26.1 (CH_2), 25.6 (CH_2), 22.1 (CH); MS (FAB$^+$/NBA) calculated for $C_{18}H_{22}NO$ (MH^+), 268.1701; found, 268.1700.

***threo*-2-[Hydroxy(1-naphthyl)methyl]quinuclidine *p*-Chlorobenzoate (8).** The crude *threo* alcohol (mother liquor from the above experiment, 1.86 g, 6.96 mmol) was dissolved in CH_2Cl_2 (25 mL), and pyridine (0.57 mL, 7.05 mmol) was added, followed by *p*-chlorobenzoyl chloride (0.95 mL, 7.44 mmol). The solution was stirred overnight, and the reaction was quenched with water (1.0 mL). After 30 min, aqueous K_2CO_3 (ca. 2 M, 80 mL) was added and the mixture extracted with CH_2Cl_2 (3 × 80 mL). The combined extracts were dried (K_2CO_3) and evaporated. Recrystallization from ethyl acetate/hexane gave the title compound **8** (2.31 g, 82%) as colorless, small prisms: mp 173 °C; IR (KBr) ν 3049 (w), 3014 (w), 2943 (m), 2863 (m), 1708 (s), 1594 (m), 1272 (s), 1100 (m), 957 (m), 807 (m), 756 (m) cm^{-1}; ^1H NMR δ 8.52 (d, J = 8.6, 1H), 7.99 (d, J = 8.7, 2H), 7.88 (dd, J = 0.5, 8.1, 1H), 7.83 (d, J = 8.2, 1H), 7.70 (dd, J = 0.6, 6.7, 1H), 7.63 (ddd, J = 1.4, 6.8, 8.6, 1H), 7.55–7.46 (m, 2H), 7.35 (d, J = 8.7, 2H), 6.81 (br d, J = 8.9, 1H), 3.69 (q, J = 9.3, 1H), 3.38 (dt, J = 13.7, 8.6, 1H), 3.08–2.93 (m, 2H), 2.89–2.79 (m, 1H), 1.67 (br s, 1H), 1.56–1.40 (m, 4H), 1.20–1.10 (m, 1H), 1.02–0.94 (m, 1H); ^{13}C NMR δ 165.3 (CO), 139.0 (Cq), 133.9 (Cq), 133.8 (Cq), 131.7 (Cq), 131.2 (2CH), 129.0 (CH), 128.9 (CH), 128.4 (2CH), 126.5 (CH), 125.6 (CH), 125.2 (CH), 123.6 (CH), 73.2 (br, CH), 59.8 (CH), 49.8 (CH_2), 42.0 (CH_2), 29.8 (CH_2), 26.7 (CH_2), 25.5 (CH_2), 21.6 (CH); MS (FAB$^+$/NBA) calculated for $C_{25}H_{25}ClNO_2$ (MH^+), 406.1574; found, 406.1570. Anal. Calcd for $C_{25}H_{24}ClNO_2$: C, 73.97; H, 5.96; N, 3.45. Found: C, 73.73; H, 5.83; N, 3.37.

***erythro*-2-[Hydroxy(1-naphthyl)methyl]quinuclidine *p*-Chlorobenzoate (9).** Pyridine (0.27 mL, 3.3 mmol) and *p*-chloroben-

zoyl chloride (0.44 mL, 3.46 mmol) were added to a suspension of *erythro*-2-[hydroxy(1-naphthyl)methyl]quinuclidine (0.87 g, 3.24 mmol) in CH_2Cl_2 (10 mL). After 1 h, a clear solution had formed and the reaction was quenched with water (0.5 mL). The mixture was stirred for 30 min and then poured into aqueous K_2CO_3 (ca. 2 M, 50 mL) and extracted with CH_2Cl_2 (3 × 50 mL). The combined extracts were dried (K_2CO_3) and evaporated. Purification of the residue by flash chromatography (silica gel, ethyl acetate/ethanol/Et_3N, 94:4:2), followed by recrystallization from ethyl acetate/hexane gave the title compound **9** (1.04 g, 79%) as colorless, small prisms: mp 166–167 °C; IR (KBr) ν 3070 (w), 2921 (m), 2860 (w), 1727 (s), 1594 (m), 1457 (m), 1270 (s), 1117 (m), 1106 (m), 1092 (m), 783 (m), 768 (s) cm^{-1}; ^1H NMR δ 8.34 (d, J = 8.5, 1H), 8.03 (d, J = 8.6, 2H), 7.86 (d, J = 8.4, 1H), 7.79 (d, J = 8.2, 1H), 7.62–7.55 (m, 2H), 7.52–7.40 (m, 4H), 6.87 (br d, J = 6.8, 1H), 3.59 (q, J = 8.1, 1H), 3.28–3.18 (m, 1H), 2.90–2.78 (m, 2H), 2.73 (ddd, J = 3.2, 10.8, 13.9, 1H), 1.91 (m, 1H), 1.85–1.72 (m, 2H), 1.70–1.60 (m, 1H), 1.58–1.46 (m, 3H); ^{13}C NMR δ 164.8 (CO), 139.5 (Cq), 135.5 (Cq), 133.9 (Cq), 131.0 (2CH), 130.7 (Cq), 129.0 (CH), 128.8 (2CH), 128.7 (CH), 126.3 (CH), 125.6 (CH), 125.2 (CH), 124.3 (Cq), 123.3 (CH), 76.4 (CH), 59.7 (CH), 50.6 (CH_2), 43.2 (CH_2), 29.2 (CH_2), 26.8 (CH_2), 25.6 (CH_2), 21.8 (CH); MS (FAB$^+$/NBA) calculated for $C_{25}H_{25}ClNO_2$ (MH^+), 406.1574; found, 406.1570. Anal. Calcd for $C_{25}H_{24}ClNO_2$: C, 73.97; H, 5.96; N, 3.45. Found: C, 73.88; H, 5.95; N, 3.30.

***erythro*-2-[Hydroxy(4-quinolyl)methyl]quinuclidine.** (a) Preparation of quinuclidine *N*-oxide: Hydrogen peroxide (30%, 6.0 g) was added to a stirred solution of quinuclidine (5.2 g, 46.77 mmol) in methanol (10.0 mL) with ice cooling. After 1 h, the solution was allowed to warm to room temperature (the reaction temperature was controlled carefully and kept below 30 °C by cooling occasionally). The mixture was allowed to stand at room temperature for 3 days until a phenolphthalein test on a small sample showed absence of quinuclidine. A spatula tip of 10% Pt on charcoal was added and the mixture stirred for 12 h, to destroy excess H_2O_2. The solution was evaporated *in vacuo* and the residue dried under high vacuum at 40 °C for 4 days, to give quinuclidine *N*-oxide (6.07 g) as a very hygroscopic, colorless solid. The compound was handled under argon and used for the next step without delay.

(b) Condensation of quinoline-4-carboxaldehyde and quinuclidine *N*-oxide: Powdered quinuclidine *N*-oxide (5.96 g, 46.9 mmol) was partially dissolved in a mixture of tetramethylethylenediamine (7.8 mL, 51.7 mmol) and THF (250 mL) under argon at room temperature. After the mixture was cooled to −78 °C, *n*-butyllithium (2.5 M solution in hexanes, 21.0 mL, 52.5 mmol) was added slowly to the vigorously stirred mixture, causing the solids to dissolve slowly. After 1 h, a solution of the quinoline-4-carboxaldehyde (8.3 g, 52.8 mmol) in THF (20 mL) was added rapidly and stirring was continued at −78 °C for 1 h. The reaction was allowed to warm to room temperature for 1 h and then quenched by careful addition of saturated aqueous NH_4Cl (80.0 mL). The *N*-oxide was reduced *in situ* by addition of a freshly prepared, concentrated solution of $TiCl_3$ in 2 N HCl, until the aqueous layer stayed slightly purple, due to excess reagent (requires ca. 20 g of $TiCl_3$). The mixture was adjusted to ca. pH 10 by addition of 15% aqueous NaOH, and stirring was continued until the solids had turned light gray. The mixture was filtered through Celite and the residue washed with ether (ca. 4 × 100 mL). The filtrate was dried (K_2CO_3) and evaporated *in vacuo* to obtain an orange gum. Filtration through a pad of silica gel (gradient elution, CH_2Cl_2/MeOH/Et_3N, 90:10:1 to 80:20:1) gave a 1:1 mixture of the crude, diastereomeric alcohols as a yellow solid (8.63 g, 69%). The crude product was recrystallized from ethyl acetate/ethanol to obtain the pure *erythro* alcohol (2.46 g) as a colorless powder. A further amount of product was obtained by concentrating the mother liquor (total: 2.75 g, 22%). The relative stereochemistry was confirmed by single-crystal X-ray diffraction of the *p*-chlorobenzyl ester (supplementary material). Physical data: mp 225 °C; IR (KBr) ν 3000–2300 (br, OH), 3064 (w), 2933 (m), 2871 (m), 1592 (m), 1569 (w), 1509 (m), 1453 (m), 1123 (m), 814 (m), 756 (s) cm^{-1}; ^1H NMR δ 8.89 (d, J = 4.5, 1H), 8.11 (dd, J = 0.8, 8.5, 1H), 7.87 (d, J = 8.3, 1H), 7.68 (d, J = 4.5, 1H), 7.64 (ddd, J = 1.2, 6.9, 8.5, 1H), 7.33 (t, J = 7.4, 1H), 5.84 (br s, 2H), 3.67–3.56 (m, 1H), 3.07 (t, J = 8.6, 1H), 2.87 (ddt, J = 9.9, 12.6, 2.8, 1H), 2.67 (ddd, J = 7.4, 9.8, 13.3, 1H), 2.36–2.26 (m, 1H), 1.95–1.86 (m, 1H), 1.80 (br s, 1H), 1.66–1.55 (m, 1H), 1.46–1.28 (m, 3H), 1.20–1.11 (m, 1H); ^{13}C NMR δ 150.5 (Cq), 150.0 (CH), 148.0 (Cq), 130.1 (CH), 128.9 (CH), 126.4 (CH), 125.3 (Cq), 122.7 (CH), 118.1 (CH), 70.8 (CH), 59.5 (CH), 50.3 (CH_2), 43.7 (CH_2), 25.9 (CH_2), 25.2 (CH_2), 24.4 (CH_2), 21.7 (CH); MS (FAB$^+$/NBA) calculated for $C_{17}H_{21}N_2O$ (MH^+), 269.1654; found, 269.1650. Anal. Calc for $C_{17}H_{20}N_2O$: C, 76.09; H, 7.51; N, 10.44. Found: C, 75.92; H, 7.45; N, 10.34.

***erythro*-2-[Hydroxy(4-quinolyl)methyl]quinuclidine *p*-Chlorobenzoate (7).** Pyridine (0.6 mL, 7.41 mmol) was added to a stirred suspension of *erythro*-2-[hydroxy(4-quinolyl)methyl]-quinuclidine (2.0 g, 7.45 mmol) in CH_2Cl_2 (35.0 mL), followed by *p*-chlorobenzoyl chloride (1.02 mL, 8.03 mmol). The starting material completely dissolved in the course of the reaction. After 4 h, water (1.0 mL) was added and stirring was continued for an additional 30 min. The mixture was poured into aqueous K_2CO_3 (ca. 2 M, 50 mL) and extracted with CH_2Cl_2 (3 × 60 mL). The combined organic layers were dried (K_2CO_3) and evaporated *in vacuo*. Purification by flash chromatography (silica gel, gradient elution: ethyl acetate/ethanol/Et_3N, 90:8:2 to 83:15:2) followed by recrystallization from ethyl acetate/hexane gave the ester **7** (2.58 g, 85%) as a colorless powder. Suitable crystals for single-crystal X-ray diffraction were grown from acetone: mp 169–170 °C; IR (KBr) ν 3070 (w), 2933 (m), 2861 (m), 1725 (s), 1594 (s), 1571 (m), 1508 (m), 1272 (s), 1104 (s), 756 (s), 683 (m), 519 (m) cm^{-1}; ^1H NMR δ 8.87 (d, J = 4.5, 1H), 8.30 (d, J = 8.1, 1H), 8.13 (dd, J = 0.6, 8.4, 1H), 8.02 (d, J = 8.6, 2H), 7.73 (dt, J = 1.2, 7.6, 1H), 7.63 (dt, J = 1.2, 7.7, 1H), 7.48–7.42 (m, 3H), 6.79 (d, J = 6.9, 1H), 3.53 (q, J = 8.2, 1H), 3.26–3.15 (m, 1H), 2.88–2.78 (m, 2H), 2.74 (ddd, J = 4.3, 11.4, 13.5, 1H), 1.93 (m, 1H), 1.82–1.70 (m, 2H), 1.70–1.60 (m, 1H), 1.59–1.47 (m, 3H); ^{13}C NMR δ 164.7 (CO), 149.9 (CH), 148.5 (Cq), 145.2 (Cq), 139.9 (Cq), 131.0 (2CH), 130.5 (CH), 129.2 (CH), 128.9 (2CH), 128.1 (Cq), 126.9 (CH), 125.9 (Cq), 123.2 (CH), 118.4 (CH), 75.0 (CH) 59.8 (CH), 50.5 (CH_2), 43.2 (CH_2), 29.1 (CH_2), 26.7 (CH_2), 25.4 (CH_2), 21.7 (CH); MS (FAB$^+$/NBA) calculated for $C_{24}H_{24}ClN_2O_2$ (MH^+), 407.1526; found, 407.1530. Anal. Calc for $C_{24}H_{23}ClN_2O_2$: C, 70.84; H, 5.70; N, 6.88. Found: C, 70.59; H, 5.67; N, 6.74.

2-(Hydroxymethyl)quinuclidine *p*-Chlorobenzoate (12). 4-Chlorobenzoyl chloride (2.79 mL, 21.95 mmol) was added to a solution of 2-(hydroxymethyl)quinuclidine[11] (2.95 g, 20.9 mmol) and pyridine (1.7 mL, 21.1 mmol) in CH_2Cl_2 (25 mL). The reaction mixture was stirred at room temperature until TLC (MeOH/ethyl acetate/NH_4OH, 9:90:1) showed absence of starting material. The reaction mixture was poured into aqueous K_2CO_3 (2 M, 80 mL) and extracted with CH_2Cl_2 (3 × 80 mL). The combined extracts were dried (K_2CO_3) and evaporated *in vacuo*. The crude ester was purified by column filtration on basic Al_2O_3 (Act. I, gradient elution: 75% ether/hexane, then neat ether) to obtain the title compound as a colorless oil (5.1 g, 87%), which solidified on standing: mp 50 °C; IR (neat) ν 3097 (w), 2943 (m), 2861 (m), 1715 (s), 1593 (m), 1488 (m), 1401 (m), 1270 (s), 1121 (m), 1088 (m), 758 (m) cm^{-1}; ^1H NMR δ 7.94 (d, J = 8.5, 2H), 7.35 (d, J = 8.5, 2H), 4.36 (dd, J = 8.3, 11.4, 1H), 4.19 (dd, J = 5.8, 11.4, 1H), 3.26–3.15 (m, 1H), 3.06–2.96 (m, 1H), 2.95–2.89 (m, 2H), 2.73 (dddd, J = 1.1, 5.2, 9.3, 14.5, 1H),

1.82–1.67 (m, 2H), 1.55–1.39 (m, 4H), 1.14 (dd, J = 7.7, 12.7, 1H); ^{13}C NMR δ 165.8 (CO), 139.1 (Cq), 131.0 (2CH), 128.5 (Cq), 128.5 (2CH), 66.2 (CH_2), 54.5 (CH), 49.6 (CH_2), 41.8 (CH_2), 29.8 (CH_2), 26.6 (CH_2), 25.5 (CH_2), 21.3 (CH); MS (FAB$^+$/NBA) calculated for $C_{15}H_{19}ClNO_2$ (MH^+), 280.1104; found, 280.1105.

2-Benzylidene-3-quinuclidinone. 3-Quinuclidinone (3.54 g, 28.3 mmol) and powdered KOH (0.5 g, 8.9 mmol) were dissolved in MeOH (25 mL), and freshly distilled benzaldehyde (3 mL, 29.5 mmol) was added to the solution. The mixture was stirred at room temperature for 20 h and then diluted with H_2O (30 mL). After the mixture was cooled to 0 °C for 30 min, the yellow solid was filtered off, washed with H_2O/MeOH (2:1), and dried under vacuum, to obtain the enone (4.36 g, 72%) as a yellow solid, sufficiently pure for the next step. An analytical sample was recrystallized from ether/pentane to obtain yellow, short needles: mp 127–128 °C; IR (KBr) ν 2956 (m), 2943 (m), 2873 (m), 1704 (s), 1625 (s), 1250 (m), 1169 (s), 1098 (s), 944 (s), 689 (s) cm^{-1}; ^{1}H NMR δ 8.03 (dd, J = 1.6, 7.8, 2H), 7.43–7.3 (m, 3H), 7.02 (s, 1H), 3.16 (dt, J = 13.6, 7.8, 2H), 3.07–2.94 (m, 2H), 2.63 (quin, J = 3.0, 1H), 2.03 (t, J = 7.9, 2H), 2.02 (t, J = 7.9, 2H); MS (FAB$^+$/NBA) calculated for $C_{14}H_{16}NO$ (MH^+), 214.1232; found, 214.1236. Anal. Calc for $C_{14}H_{15}NO$: C, 78.84; H, 7.09; N, 6.57. Found: C, 79.01; H, 6.98; N, 6.55.

2-Benzyl-3-quinuclidinone. A suspension of 2-benzylidine-3-quinuclidinone (4.53 g, 21.2 mmol) in MeOH (200 mL) was hydrogenated in a Parr shaker at 50 psi over 10% Pd/C (0.3 g). After the hydrogen consumption was complete (4 h), the mixture was filtered through a pad of Celite and the pad washed with MeOH. The colorless filtrate was evaporated *in vacuo* and the residue recrystallized from EtOAc/hexane to obtain 2-benzyl-3-quinuclidinone (4.36 g, 95%) as large, colorless needles: mp 77–78 °C; IR (KBr) ν 3029 (w), 2954 (m), 2879 (w), 1721 (s), 1600 (w), 1495 (w), 1451 (m), 1079 (m), 982 (m), 760 (m), 702 (s) cm^{-1}; ^{1}H NMR δ 7.35–7.17 (m, 5H), 3.38 (dd, J = 4.0, 10.8, 1H), 3.27–3.16 (m, 1H), 3.21 (dd, J = 3.9, 14.8, 1H), 3.11 (dt, J = 13.8, 7.9, 1H), 2.93–2.82 (m, 2H), 2.78 (dd, J = 10.8, 14.8, 1H), 2.47 (quin, J = 3.0, 1H), 2.06–1.93 (m, 4H); ^{13}C NMR δ 221.2 (CO), 139.0 (Cq), 128.7 (2CH), 128.4 (2CH), 126.4 (CH), 71.5 (CH), 48.9 (CH_2), 40.9 (CH_2), 40.0 (CH), 33.6 (CH_2), 26.6 (CH_2), 25.1 (CH_2); MS (FAB$^+$/NBA) calculated for $C_{14}H_{18}NO$ (MH^+), 216.1388; found, 216.1391.

2-Benzylquinuclidine (14). Powdered KOH (3.0 g, 53.6 mmol) was added to a solution of 2-benzyl-3-quinuclidinone (4.28 g, 19.9 mmol) and hydrazine monohydrate (2.8 g, 55.9 mmol) in triethylene glycol (13.5 mL), and the mixture was heated to 150 °C. After 3.5 h, the mixture was allowed to cool to room temperature, diluted with H_2O (80 mL), and extracted with ether (4 × 60 mL). The combined extracts were washed with brine (60 mL), dried (K_2CO_3), and evaporated *in vacuo*. The product was purified *via* its *p*-toluenesulfonic acid (*p*TSA) salt, which was prepared by dissolving the crude quinuclidine in ethanol (20 mL) and adding a solution of pTSA (3.6 g, 18.9 mmol) in ethanol (20 mL). The solution was then concentrated to ca. 15 mL and warmed to ca. 35 °C, and ether was added until the solution turned slightly cloudy. The salt crystallized on cooling slowly to −15 °C for 1.5 h, and it was isolated by filtration and washing first with cold ether/ethanol (1:1) and then with neat ether to obtain a white powder (3.48 g). A further amount (0.68 g) was obtained by concentrating the mother liquor and treating it with ether as described above, to give a total amount of 4.16 g of the salt. The free base was obtained by treating the salt with a saturated aqueous Na_2CO_3 solution and extracting with ether. The combined extracts were dried (K_2CO_3) and evaporated under vacuum. Purification by vacuum distillation (×2) gave 2-benzylquinuclidine (**14**) (1.5 g, 37%) as a colorless liquid: bp 97–103 °C (0.1 mmHg); IR (neat) ν 3085 (w), 3064 (w), 3027 (m), 2912 (s), 2863 (s), 1605 (w), 1584 (w), 1497 (m), 1455 (s), 1324 (m), 988 (m), 739 (s), 698 (s) cm^{-1}; ^{1}H NMR δ 7.31–7.15 (m, 5H), 3.16–2.99 (m, 2H), 2.96–2.88 (m, 3H), 2.81–2.73 (m, 1H), 2.69 (dd, J = 9.2, 13.3, 1H), 1.75 (sept, J = 3.2, 1H), 1.62–1.43 (m, 5H), 1.19 (br dd, J = 7.2, 12.9); ^{13}C NMR δ 139.8 (Cq), 129.0 (2CH), 128.2 (2CH), 125.9 (CH), 57.4 (CH), 49.9 (CH_2), 41.8 (CH_2), 41.6 (CH_2), 33.4 (CH_2), 26.9 (CH_2), 25.5 (CH_2), 21.9 (CH); MS (FAB$^+$/NBA) calculated for $C_{14}H_{20}N$ (MH^+), 202.1596; found, 202.1600.

2-(1-Naphthylmethylene)-3-quinuclidinone. 3-Quinuclidinone (5.0 g, 39.9 mmol) and KOH (0.7 g, 12.5 mmol) were dissolved in MeOH (35 mL), and 1-naphthalenecarboxaldehyde (5.65 mL, 41.6 mmol) was added. The mixture was stirred for 24 h, during which time a yellow precipitate was formed. The mixture was diluted with H_2O (20 mL), cooled to 0 °C, and then filtered, and the residue was washed with cold H_2O/MeOH (1:1). The crude product was purified by recrystallization from ethyl acetate/hexane to obtain the enone (4.95 g, 47%) as small, thin plates: mp 145–146 °C; IR (neat) ν 2964 (m), 2935 (m), 2871 (w), 1700 (s), 1613 (s), 1331 (m), 1239 (m), 1102 (s), 772 (s) cm^{-1}; ^{1}H NMR δ 8.36 (d, J = 7.3, 1H), 8.19 (d, J = 8.5, 1H), 7.90 (s, 1H), 7.88–7.82 (m, 2H), 7.59–7.47 (m, 3H), 3.25–3.14 (m, 2H), 3.10–2.98 (m, 2H), 2.70 (quin, J = 3.0, 1H), 2.13–2.01 (m, 4H); MS (FAB$^+$/NBA) calculated for $C_{18}H_{18}NO$ (MH^+), 264.1388; found, 264.1389. Anal. Calc for $C_{18}H_{17}NO$: C, 82.10; H, 6.51; N, 5.32. Found: C, 82.00; H, 6.55; N, 5.39.

2-(1-Naphthylmethyl)-3-quinuclidinone. A suspension of 2-(1-naphthylmethylene)-3-quinuclidinone (4.93 g, 18.7 mmol) and 10% Pd/C (0.3 g) in MeOH (200 mL) was hydrogenated in a Parr apparatus at 50 psi. After the hydrogen consumption was complete (4 h), the mixture was filtered through a pad of Celite and the pad was washed with MeOH. The solution was evaporated *in vacuo* to obtain a viscous, yellow oil. The crude product was purified via its HBr salt by dissolving it in MeOH (20 mL) and adding 48% aqueous HBr (3.2 g, ca. 19.5 mmol). The solution was evaporated *in vacuo* and the residue recrystallized from ethanol at reflux. The HBr salt completely precipitated on cooling slowly to −20 °C, and it was filtered off and washed with cold ethanol, followed by ether, to obtain a colorless solid (4.91 g). The free base was obtained by treating the salt with a saturated aqueous K_2CO_3 solution (100 mL) and extracting with ether (4 × 50 mL). The combined extracts were washed with brine (50 mL), dried (K_2CO_3), and evaporated under vacuum to obtain the quinuclidinone as a yellowish oil (3.79 g, 76%), which solidified on standing: mp 81–82 °C; IR (neat) ν 3051 (w), 2958 (m), 2877 (m), 1721 (s), 1600 (m), 1509 (m), 1463 (m), 1084 (s), 1073 (s), 799 (s), 778 (s) cm^{-1}; ^{1}H NMR δ 8.15 (br d, J = 8.2, 1H), 7.86 (br d, J = 8.8, 1H), 7.78–7.71 (m, 1H), 7.54 (ddd, J = 1.5, 6.8, 8.4, 1H), 7.48 (ddd, J = 1.3, 6.8, 8.0, 1H), 7.45–7.38 (m, 2H), 3.78 (dd, J = 3.7, 14.9, 1H), 3.54 (dd, J = 3.5, 9.8, 1H), 3.42–3.30 (m, 1H), 3.13 (dd, J = 9.8, 14.9, 1H), 3.12–3.04 (m, 1H), 2.98–2.88 (m, 1H), 2.87–2.77 (m, 1H), 2.52 (quin, J = 3.0, 1H), 2.08 (dt, J = 2.9, 8.0, 2H), 2.00–1.93 (m, 2H); ^{13}C NMR δ 221.4 (CO), 135.0 (Cq), 133.9 (Cq), 131.6 (Cq), 128.9 (CH), 127.2 (CH), 127.0 (CH), 126.1 (CH), 125.52 (CH), 125.46 (CH), 123.4 (CH), 70.6 (CH), 48.8 (CH_2), 41.3 (CH_2), 40.1 (CH), 31.1 (CH_2), 26.9 (CH_2), 24.9 (CH_2); MS (FAB$^+$/NBA) calculated for $C_{18}H_{20}NO$ (MH^+), 266.1545; found, 266.1541. Anal. Calc for $C_{18}H_{19}NO$: C, 81.47; H, 7.22; N, 5.28. Found: C, 81.24; H, 7.10; N, 5.15.

2-(1-Naphthylmethyl)quinuclidine (15). Powdered KOH (1.9 g, 33.9 mmol) was added to a solution of 2-(1-naphthylmethyl)-3-quinuclidinone (3.62 g, 13.7 mmol) and hydrazine monohydrate (1.9 g, 38.0 mmol) in triethylene glycol (9.5 mL), and the mixture was heated at 160 °C for 4 h. After being cooled to room temperature, the reaction mixture was diluted with H_2O (80 mL) and extracted with ether (3 × 60 mL). The combined extracts were washed with brine (70 mL), dried (K_2CO_3), and evaporated *in vacuo*. The product was purified via its pTSA salt, which was

prepared by adding *p*TSA monohydrate (2.5 g, 13.1 mmol) to a solution of the crude quinuclidine in ethanol (15 mL) and evaporating to dryness. The salt was recrystallized from hot ethanol (15 mL) by adding ether until the solution turned cloudy and cooling slowly to −15 °C. The solid was filtered off, washed with ether/ethanol (1:1), followed by ether, and dried under vacuum to give a colorless powder (4.61 g), which was treated with a saturated aqueous solution of Na_2CO_3 and extracted with ether. The combined extracts were washed with brine, dried (K_2CO_3), and evaporated *in vacuo*. Vacuum distillation gave the pure quinuclidine (**15**) (1.64 g, 48%) as a yellowish oil: bp 150 °C (0.1 mmHg); IR (neat) ν 3047 (w), 2937 (s), 2861 (m), 1598 (w), 1509 (w), 1455 (m), 986 (m), 780 (s) cm^{-1}; ^1H NMR δ 8.10 (d, J = 8.4, 1H), 7.86 (br d, J = 8.6, 1H), 7.73 (d, J = 7.9, 1H), 7.55–7.45 (m, 2H), 7.42–7.34 (m, 2H), 3.47 (dd, J = 4.8, 13.4, 1H), 3.32–3.17 (m, 2H), 3.07 (dd, J = 9.5, 13.4, 1H), 3.00–2.90 (m, 2H), 2.89–2.79 (m, 1H), 1.76 (sept, J = 3.1, 1H), 1.63–1.36 (m, 5H), 1.31 (ddt, J = 7.2, 12.9, 2.3, 1H); ^{13}C NMR δ 135.5 (Cq), 133.9 (Cq), 132.1 (Cq), 128.7 (CH), 126.8 (2CH), 125.8 (CH), 125.4 (CH), 125.3 (CH), 123.8 (CH), 56.2 (CH), 49.9 (CH_2), 41.8 (CH_2), 39.2 (CH_2), 33.5 (CH_2), 26.9 (CH_2), 25.5 (CH_2), 21.9 (CH); MS (FAB$^+$/NBA) calculated for $C_{18}H_{22}N(MH^+)$, 252.1752; found, 252.1750.

2-Isopropyl-3-quinuclidinone. Methyllithium (38 mL of a 1.4 M solution in ether, 53 mmol) was added to a stirred suspension of CuCN (2.35 g, 26.2 mmol) in anhydrous ether (22 mL) under argon at −78 °C. The mixture was warmed to 0 °C for 10 min and then recooled to −78 °C, and a solution of 2-ethylidene-3-quinuclidinone[10] (2.5 g, 16.5 mmol) in dry ether (15 mL) was added via cannula, causing the solution to turn yellow. After 1 h at −78 °C, the reaction was warmed to 0 °C and quenched by careful addition of saturated aqueous NH_4OH/NH_4Cl (2:1) and then warmed to room temperature and diluted further with the NH_4OH/NH_4Cl buffer (ca. 70 mL). The mixture was extracted with ether (3 × 80 mL), and the combined organic layers were washed with brine (50 mL), dried (K_2CO_3), and evaporated. Bulb-to-bulb vacuum distillation gave the pure quinuclidinone (2.56 g, 93%) as a colorless liquid: bp 100 °C (0.1 mmHg, Kugelrohr); IR (neat) ν 2958 (s), 2873 (s), 1721 (s), 1472 (m), 1457 (m), 1069 (m), 1042 (m), 841 (m) cm^{-1}; ^1H NMR δ 3.10–2.98 (m, 2H), 2.85–2.73 (m, 2H), 2.61 (d, J = 10.1, 1H), 2.34 (quin, J = 3.0, 1H), 1.99–1.85 (m, 5H), 1.14 (d, J = 6.5, 3H), 1.00 (d, J = 6.6, 3H); ^{13}C NMR δ 221.4 (CO), 75.5 (CH), 49.0 (CH_2), 41.1 (CH_2), 40.7 (CH), 28.2 (CH), 27.1 (CH_2), 24.7 (CH_2), 21.5 (CH_3), 20.8 (CH_3); MS (FAB$^+$/NBA) calculated for $C_{10}H_{18}NO$ (MH^+), 168.1388; found, 168.1390.

2-Isopropylquinuclidine. KOH (1.4 g, 25.0 mmol) and 2-isopropyl-3-quinuclidinone (1.67 g, 10.0 mmol) were dissolved in triethylene glycol (7.0 mL), and hydrazine monohydrate (1.4 g, 28.0 mmol) was added. The mixture was heated to 150–160 °C for 3 h and then cooled to room temperature, diluted with H_2O (50 mL), and extracted with ether (3 × 70 mL). The combined extracts were washed with brine (50 mL), dried (K_2CO_3), and evaporated to obtain the crude product as a colorless liquid (1.06 g). For further purification, the crude quinuclidine was dissolved in ethanol (15 mL) and neutralized with *p*TSA monohydrate (1.6 g, 8.4 mmol). The solution was concentrated until crystallization just started; then it was warmed to ca. 40 °C, and ether was added until the mixture was slightly turbid. The solution was cooled slowly to 0 °C and then filtered, and the residue was washed with cold ether/ethanol (2:1) and dried under vacuum. The salt was treated with aqueous Na_2CO_3 (ca. 2 M, 50 mL), and the mixture extracted with ether (3 × 50 mL). The combined extracts were washed with brine (50 mL), dried (K_2CO_3), and evaporated. Bulb-to-bulb vacuum distillation of the residue gave 2-isopropylquinuclidine (0.96 g, 63%) as a colorless liquid: bp 120 °C (ca. 15 mmHg, Kugelrohr); IR (neat) ν 2933 (s), 2867 (s), 1457 (m), 1318 (m), 1069 (m), 1050 (m), 1011 (m), 810 (m) cm^{-1}; ^1H NMR δ 3.0–2.8 (m, 3H), 2.65 (dddd, J = 1.3, 5.0, 10.1, 13.6, 1H), 2.15 (br q, J = 9.0, 1H), 1.77–1.68 (m, 2H), 1.57 (ddt, J = 10.3, 13.1, 6.5, 1H), 1.49–1.33 (m, 4H), 1.17–1.07 (m, 1H), 0.94 (d, J = 6.5, 3H), 0.88 (d, J = 6.6, 3H); ^{13}C NMR δ 63.0 (CH), 50.0 (CH_2), 41.4 (CH_2), 33.5 (CH_2), 32.6 (CH), 27.0 (CH_2), 25.8 (CH_2), 22.0 (CH), 21.0 (CH_3), 19.6 (CH_3); MS (FAB$^+$/NBA) calculated for $C_{10}H_{20}N$ (MH^+), 154.1596; found, 154.1600.

Acknowledgment. This work was supported by the National Institutes of Health (Grant GM 28384) and the National Science Foundation (Grant CHE-8903218). H.C.K. thanks the Deutsche Forschungsgemeinschaft and GLAXO Research for fellowships. We are grateful to P.-O. Norrby for providing the UV-binding program and P. Ganzel of University of California, San Diego, for the X-ray crystal structures of ligands **6** and **7**. We thank S. Loren and P.-O. Norrby for helpful discussions.

Supplementary Material Available: Tables containing kinetic data and saturation plots with $(DHQD)_2PHAL$ and 1-decene and X-ray data for ligands **6** and **7** (20 pages). This material is contained in many libraries on microfiche, immediately follows this article in the microfilm version of the journal, and can be ordered from the ACS; see any current masthead page for ordering information.